



Remote sensing and interdisciplinary approach for forecasting and analysing the effects of hurricanes, tropical cyclones and typhoons

Maurizio Fea^a, Massimo Capaldo^b, Cristiano Pesaresi^c

^a Italian Geophysics Association, Rome, Italy

^b Italian Meteorological Service, Rome, Italy

^c Dipartimento di Scienze documentarie, linguistico-filologiche e geografiche, Sapienza University of Rome, Rome, Italy

Email: maufea@gmail.com

Received: April 2015 – Accepted: May 2015

Abstract

Hurricanes, tropical cyclones and typhoons are feared phenomena which frequently cause dramatic damage and consequences in different areas of the world. Since their impact typologies are very different according to the human and social contexts in which they break out, after providing a framework on their main characteristics, structures and measuring scales, we provide some considerations regarding the possible kinds of human works and elements which can be involved and the resilience of the populations. Then, we focus the attention on essential aspects to interpret satellite and radar imagery in order to support the observation and forecast of hurricanes, tropical cyclones and typhoons. Thus, we provide numerous pieces of evidence regarding the importance and the added value of remote sensing in recent events as far as concerns for example the possibilities to: monitor the formation and development of these phenomena; estimate their maximum intensity and their turbulence intensity; provide useful indications for civil protection measures and activities; evaluate the amount of damage caused on many components, in terms of ecosystems and anthropic structures; quantify the land use changes between pre and post events; determine the general impact on urban areas and coastal zones etc. As different exemplificative cases for a specific analysis supported by the geomatics interpretation of remote sensing imagery, we have chosen: Hurricane Katrina, for the amount of widespread damage caused; Typhoon Haiyan, also known as Super-Typhoon Haiyan; and Typhoon Tip, considered to be the largest typhoon that ever occurred. According to the scheme defined by previous contributions (Fea et al., 2013a, 2013b), we also provide some didactical input for a participative and critical study of these phenomena, where students can converge methodological and applicative aptitudes, thus becoming actively responsible of their learning process.

Keywords: Damages, Forecast, GIS, Hurricanes, Tropical Cyclones and Typhoons, Remote Sensing, Satellite and Aerial Imagery

1. Introduction

On 12 March 2015 the islands of the Republic of Vanuatu in the south-western part of the Pacific Ocean were struck by one of the strongest tropical storms that have ever been recorded. When considering examples of extreme events within the environmental framework a special place is held by tropical storms and hurricanes.

Before analysing the nature of these events, it is important to note that cyclones, hurricanes and typhoons are basically just different names for the same extreme weather phenomena in different parts of the world tropics. These storms are called *hurricanes* in the Atlantic and north-east Pacific, *typhoons* in the north-west Pacific and *cyclones* in the south Pacific and Indian Ocean. They are rightly identified as extreme natural phenomena. In order to better understand the amount of energy that is involved in the life of these storms it is useful to report that a fully developed hurricane is estimated to release heat energy at a rate of 5 to 20×10^{10} Kwatt. Such a rate of heat release is equivalent to a 10 megaton (4.2×10^{16} Joule) nuclear bomb exploding every 20 minutes. A hurricane, a cyclone or a typhoon is a sustained intensification of a pre-existing perturbation of a usual weather pattern occurring in the tropical regions. This perturbation is marked by a warm-core intense low-pressure weather system at synoptic scale (around 1000 km), a closed surface wind circulation around it (counter clockwise in the northern Hemisphere) and a strong convection pattern. Whenever such a tropical cyclone obtains a maximum sustained wind speed greater than or equal to 119 km/h, it is reclassified as a hurricane or a typhoon depending upon the region of formation¹. Mature hurricanes are nearly circular in shape and are typically a few hundred kilometers in diameter.

Overall, such phenomena are luckily not very frequent and they interest tropical areas only. Figure 1 shows a 150 year climatology of cyclone occurrences. On average there are roughly 80 hurricanes per year all over the world and most of them are of moderate intensity. Looking at Figure 1, one can draw a number of interesting considerations.

First of all, it shows that hurricanes do not interest equatorial regions, regardless of the fact that intense thunderstorms occur at the Equator: that is due to the fact that the Coriolis Force,

required for the hurricanes to form, is null in that region. In actual fact, the Coriolis force, which results from the Earth's quasi-spherical shape and its rotation around its N-S axis, has a maximum at the Poles and is null at the Equator, therefore depriving hurricanes of the trigger to be born. Furthermore, from the map it is also evident that the north-east Pacific as well as the south Atlantic are free from these events. In the Pacific, this is mainly due to the presence of a cold oceanic current moving northward along the coast of Chile, Peru and Ecuador (the very same one linked to the El Niño phenomenon). A similar cold current, the Benguela Current, flows from the western coast of South Africa northward, passing Namibia and Angola and keeping those waters too cool to bring about hurricane formation. The south Atlantic waters off the eastern coast of Brazil are not favourable for hurricanes for a variety of reasons, including prevalent wind shear (variation of wind speed or direction at different altitudes), and owing to the usual presence of intense wind vertical shear over the south Atlantic².

From a temporal viewpoint, it is clear that hurricanes occur only during specific periods of the year, which are different for the two hemispheres.

In fact, once the hurricane has been triggered, it can be considered, at a first approximation, as a heat engine: it obtains its heat input from the warm humid air over the tropical ocean, and releases this heat through the condensation of water vapour into water droplets in deep thunderstorms of the eyewall and rainbands, then giving off a cold exhaust air in the upper levels of the troposphere (~12 km up).

It turns out that the vast majority of the heat released in the condensation process is used to cause rising motions in the thunderstorms and only a small portion (10%) drives the storm's horizontal winds (Marks, 2003, p. 963).

The subsequent hurricane evolution is mainly determined by the conditions it encounters along its track over the sea, and the track itself is the result of its movement steered by larger-scale, global atmospheric circulation. Finally, as soon as hurricanes make landfall, that is to say they move from the ocean over land, they start to decay. From their internal structure point of view, hurricanes are fairly coherent weather systems with a consistent outlook (Figures 2 and 3).

¹ See <http://www.hurricanescience.org/science/science/hurricanelifecycle/>.

² See <http://earthobservatory.nasa.gov/IOTD/view.php?id=7079>.

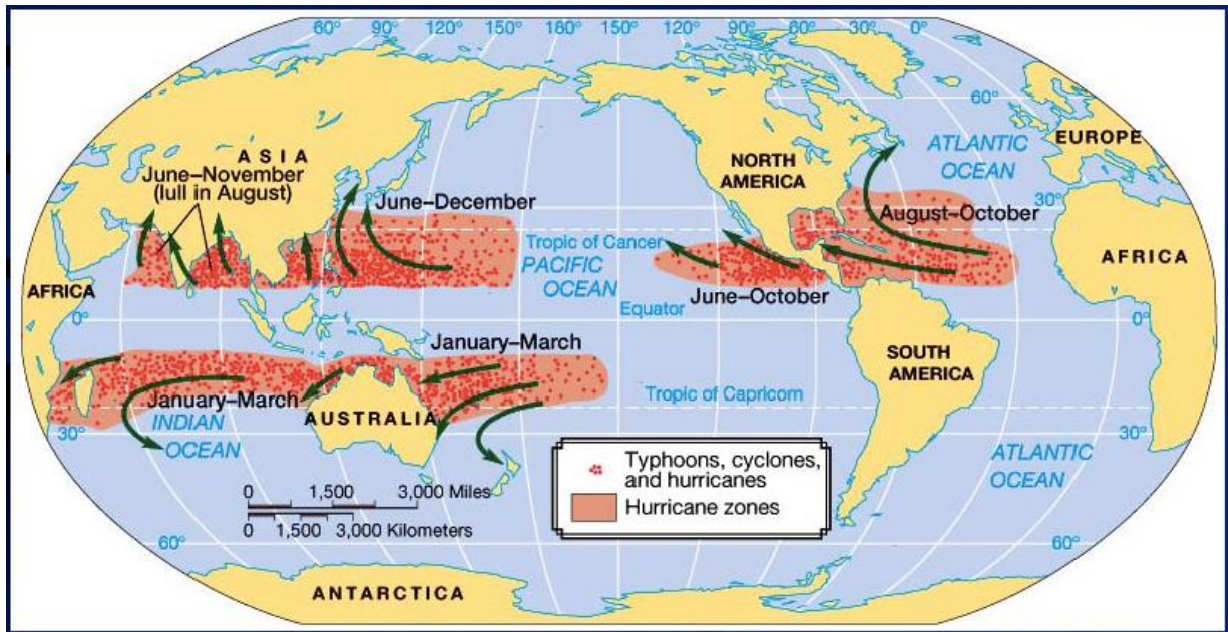


Figure 1. Climatology of tropical cyclone occurrences. Courtesy of the University of Hawaii.

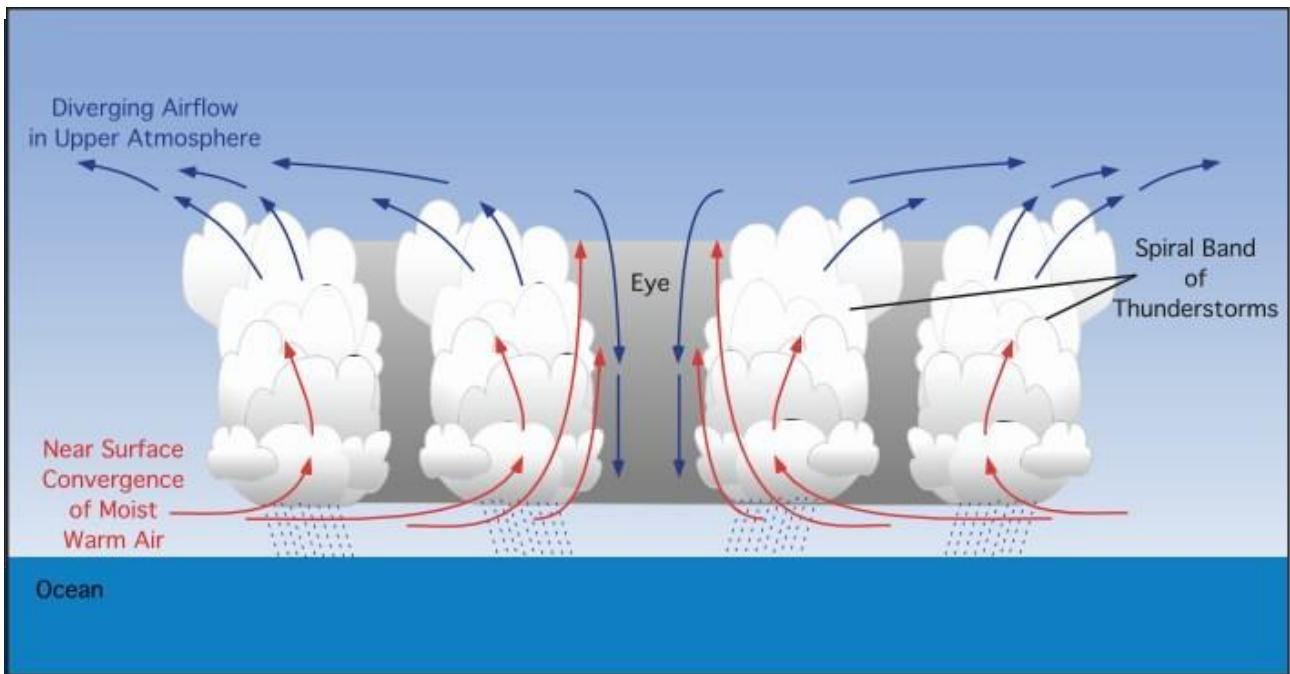


Figure 2. Hurricane structure. Courtesy of the University of British Columbia.

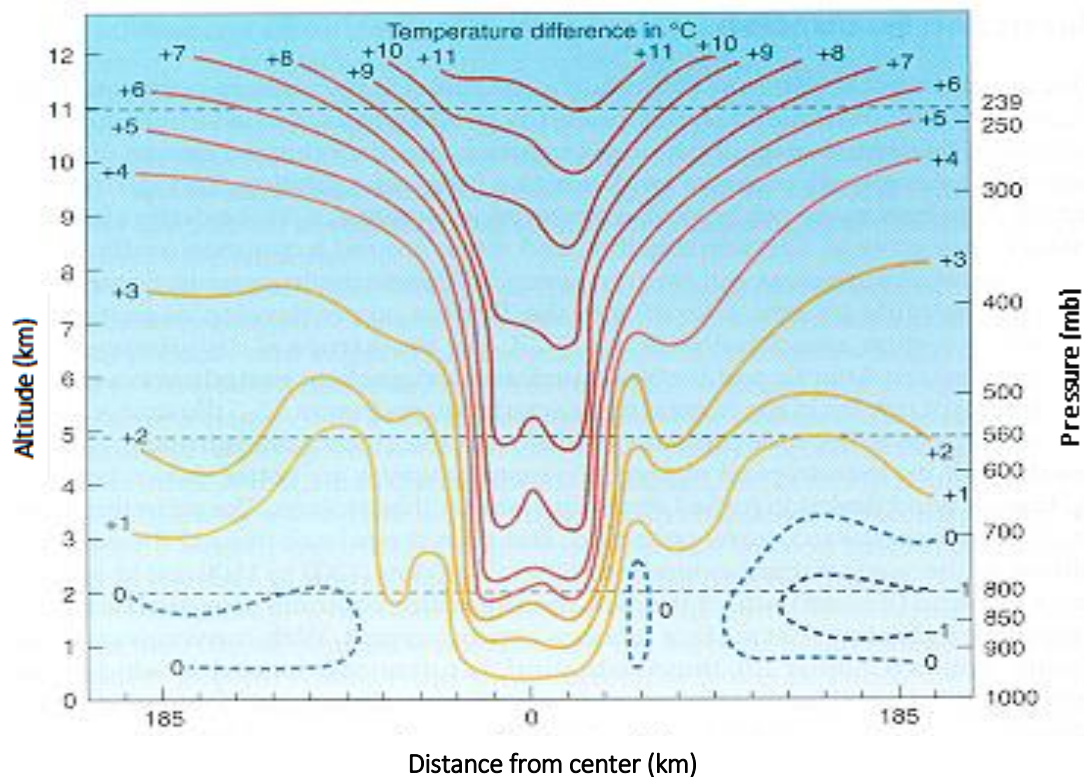


Figure 3. Vertical thermal structure of a typical hurricane. Courtesy of the University of Hawaii.

Type	Category	Pressure	Winds			Surge
			mb	Knots	m/s	
Depression	TD	----	< 34	< 17	< 39	----
Tropical Storm	TS	----	≥ 34	≥ 17	≥ 39	----
Hurricane	1	> 980	64-82	32-40	74-95	4-5
Hurricane	2	965-980	83-95	41-45	96-110	6-8
Hurricane	3	945-964	96-112	46-53	111-130	9-12
Hurricane	4	920-944	113-134	54-64	131-155	13-18
Hurricane	5	< 920	> 134	> 64	> 155	> 18

Table 1. The Saffir-Simpson hurricane scale.

Their surface winds rotate cyclonically (counterclockwise in the northern Hemisphere). The strongest winds are located in a hurricane's eyewall, which surrounds a nearly calm eye at the storm's warm center. A hurricane's eye is typically tens of kilometers in diameter. Clouds in both the eyewall and the spiral bands outside the eyewall can produce very heavy rain.

But why are hurricanes not very frequent compared to the relatively high number of atmospheric disturbances triggered in the tropics by the intense solar radiation affecting this region?

Statistical studies performed over the observed climatology of hurricanes show that a few stringent conditions are necessary for hurricane formation. They include the following (<http://www.hurricanescience.org/science/science/hurricaneogenesis/>).

- A sea temperature of at least $\sim 26.5^{\circ}\text{C}$ to a depth of ~ 50 m, so that deep cooler water cannot easily be mixed with the surface by winds (situation of deep thermocline).
- A pre-existing disturbance with cyclonic circulation (i.e. large low-level vorticity) persisting longer than 24 hrs. As the air in the disturbance converges, its angular momentum is conserved and wind speed is due to increase.
- "A vertical temperature profile in the atmosphere that cools enough with height to support thunderstorm activity".
- "Sufficient water vapour in the middle of the troposphere. Even over the tropical oceans, dry air sometimes exists in the middle of the troposphere, and this dry air suppresses thunderstorms, preventing tropical depression formation". On the other hand, if the humidity is too high in the troposphere, the disturbance will not have the capability to moisten the air (via evaporation from the sea surface) for tropical storm genesis to occur.
- Sufficient N or S distance from the Equator, as anticipated above, for the Coriolis Force to be significant to facilitate the convergence of the air masses at the surface (usually at least 4-5 degrees in latitude).
- "Low values of vertical wind shear [variation of the wind with height] from the surface of

the Earth to the upper troposphere" (about 13 km or 8 miles up). Research shows that such a situation might favour the injection of dry air into the storm system.

The intensity of the cyclone is most often defined by the maximum sustained wind a few meters above the Earth's surface.

For tropical storms observed over the north Atlantic or eastern north Pacific, Table 1 gives a more detailed classification of tropical cyclone intensity based on sea level pressure at the centre of the storm, maximum sustained wind and storm surge.

The scaling of hurricanes (category 1 to 5) is based on the Saffir-Simpson hurricane scale. But similar scales apply for other regions of the globe (Table 1).

In summary, maximum scale (category 5) hurricanes are characterized by wind speeds in excess of 230 km/h.

One important effect of the hurricane intense wind circulation is the so-called storm surge, that is, the piling up of the water higher than the ordinary sea level. It has been shown that the sea level surge caused by a land-falling storm is proportional to the maximum sustained wind or sea level pressure at the centre of the storm. The combined effects of low pressures, high waves and local increase of sea level can dramatically take advantage of an unfavourable bathymetry to cause extensive floods in those regions affected by the hurricane landfall and consequent storm surge effect (Figure 4).

Finally, it is necessary to highlight that hurricanes are very different objects when compared with extra-tropical weather perturbations. The main differences between hurricanes and mid-latitude storms are the following.

- Winter extra-tropical storms have cold and warm fronts (sharp variations in the thermal field resulting in an asymmetric shape) and occur in the middle and high latitudes (30° - 60° N or S).
- Winter storms are generally larger having spatial scales of thousands of kilometers, much larger than the typical size of hurricanes.



Figure 4. Storm surge effect. Courtesy of the UCAR Comet Program.

- The mid-latitude storms are mainly triggered and driven by three-dimensional temperature and mass variations in space, while hurricanes draw their energy from the latent heat released by the condensation of moisture due to the evaporation from the sea.
- Hurricanes have a vertical structure different from mid-latitude storms, as they have warm (not cold) core central lows and winds reduce with height. In addition, jet streams are not present aloft over hurricanes, while they are characteristic of the mid-latitude perturbations.

2.1 Observing hurricanes

In the past, it was difficult to track tropical cyclones, since these storms usually spend the majority of their life on the open ocean, far from the network of land-based weather observations: for those that never made landfall, sometimes their entire life cycle would have been completely undetected.

Today, worldwide, hurricanes and typhoons are analysed primarily with imagery from Earth Observation (EO) satellites. Prime data sources are the geostationary meteorological satellites of

the World Weather Watch: they fly at an altitude of 35,800 km in an equatorial orbit with the same angular velocity as the Earth, thereby continuously observing the same wide sector of the planet surface. Therefore, their sensors can acquire imagery data of tropical storms with extremely high time frequency and in different spectral bands simultaneously. In particular, data acquired in the thermal infrared band provides the temperature of sea surface and cloud tops, measured by sensing the thermal infrared radiation emitted by them.

In addition, EO satellites flying in near-polar orbits at altitudes in the 500-1,000 km range provide detailed storm images in the Visible, Infrared and Microwave spectral bands when they overfly it. Similarly, storm pictures are taken by astronauts from the International Space Station (ISS).

It is important to note that meteorological satellites also carry instruments that collect data that allow the generation of vertical atmospheric profiles of key geophysical parameters, such as air temperature and humidity, which are used as input information in the numerical atmospheric models for weather and storm analysis and forecast.

Together with satellites, sophisticated arrays of airborne instruments collect large quantities of high-quality data, which are taken back (or sent via satellite telecommunications) to the centres responsible and incorporated into hurricane prediction models. Furthermore, hurricane reconnaissance reports come primarily from the so-called Hurricane Hunters (Figure 5).



Figure 5. Hurricane Hunter. Courtesy of NOAA.

Original EO data are visualised by assigning a grey tone to each radiometric data value that is related to its actual value according to a defined scale, normally from black (minimum value) to white (maximum value), except for meteorological thermal and water vapour infrared imagery, where the scale is the opposite (minimum appears white and maximum black). In order to enhance the specific characteristics of a parameter very often a colour scale is applied, whereby the final coloured image depicts that characteristic. For example, the colour scale associated with different values of the sea surface temperature (SST) permits the visualisation of the horizontal distribution of SST values for an immediate detection of warm and cold waters in an SST satellite image. Similarly, a coloured satellite image of thermal infrared cloud top radiometric values shows at a glance where the coldest cloud tops are located: taking into account that the atmospheric temperature decreases with height, the coldest cloud top values indicate the location of the highest cloud tops, normally associated not only with the most dangerous thunderstorm clouds, the so-called cumulonimbus, but also where the most active cloud rain cells are located.

“Ships and buoys are other types of observational platforms that provide critical infor-

mation about the conditions within a tropical cyclone”. They “are the only routine source of measured waves in areas unobstructed by land and are often the only way to take direct measurements when a tropical system is at sea”. Furthermore, they are also used to validate “indirect measurements (such as those taken by satellites and radar)”³.

Land-based surface observations of hurricanes, such as radar (Figure 6), are invaluable sources of real-time information at both inland and coastal locations. Rainfall reports show where significant rainfall is occurring and provide the basis for flood alerts. During a hurricane’s landfall, data from satellites and reconnaissance aircrafts are compared and verified against data transmitted in real-time from weather stations located near or at the coast.

2.2 Forecasting hurricanes

All acquired datasets are the basis for forecast and warning products issued by worldwide hurricane forecast centres. These observations are checked for quality, examined and fed into a suite of analysis and forecast models, which are objective tools, usually based on mathematical models and equations, “designed to predict the future behavior of a hurricane (or more generally, any tropical cyclone). The primary purpose of a hurricane forecast model is to predict a hurricane’s track and/or intensity (and sometimes rainfall) for the next 3-5 days (although longer lead times are possible). Other forecast models are designed specifically to forecast the impacts of hurricanes, such as storm surge”⁴.

Results from the hurricane forecast models provide essential information on the estimated intensity of the storm and its likely track in the days to come. Forecast and warning products disseminated by the responsible hurricane forecasting centres allow authorities and their local emergency managers to make plans and to take actions for securing people and properties already in the days and hours prior to a hurricane landfall.

³ See <http://www.hurricanescience.org/science/observation/ships/>.

⁴ See <http://www.hurricanescience.org/science/forecast/models/>.

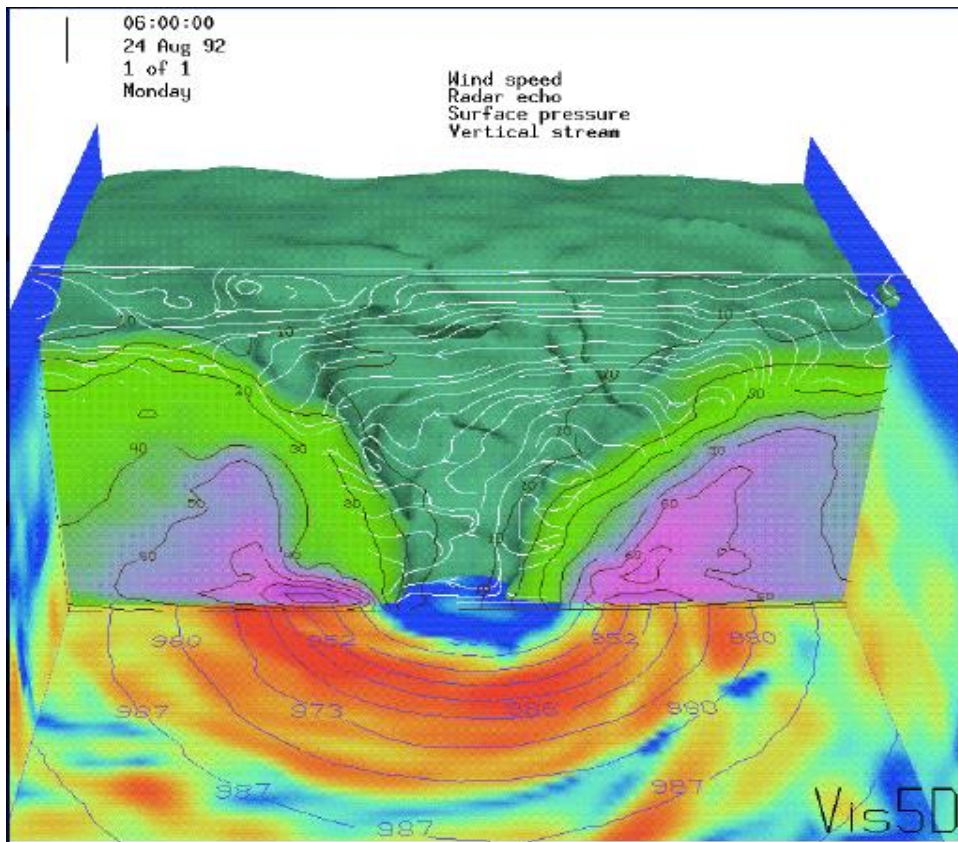


Figure 6. Hurricane Andrew (1992). The radar echo shows in purple the heavy rain band, while isobars at the surface have been drawn to depict the low pressure centre. The intense surface wind speed has been represented in red. The vertical stream isolines are also depicted. Courtesy of the University of Hawaii.

2.3 Climate effects

The most recent paper of the Intergovernmental Panel for Climate Change (IPCC) has further confirmed that global warming has to be considered a most certain outlook of the Earth's climate over the next decades.

Is such a consolidated climate evolution projecting specific effects over hurricane frequency and intensity?

So far there is no scientific consensus on how to answer to such a question.

The warming of the oceans, from which tropical storms get their primeval source of energy, would seem to imply that they would get stronger, and perhaps also more frequent. Indeed, the potential intensity of tropical storms does increase with warmer sea-surface temperatures.

However, the effect of warming seas could be counteracted by the apparent increase in the strength of wind shear that tends to hinder the

formation of storms, or tear them apart before they can reach an extreme strength.

Nevertheless, some evidence exists that storm intensity has indeed increased, but it is limited to the north Atlantic, where observations are most abundant. In other places, the available information is not yet conclusive.

On this, the Intergovernmental Panel on Climate Change (IPCC) is cautioning that:

Time series of cyclone indices, such as power dissipation, an aggregate compound of tropical cyclone duration, frequency and intensity that measures total wind energy by tropical cyclones, show since the late 1970s upward trends in the north Atlantic and weaker upward trends in the western north Pacific, but interpretation of longer-term trends is again constrained by data quality concerns (IPCC, 2013)⁵.

⁵ See also Emanuel, 2007.

3. Considerations on the impact typologies caused by hurricanes, tropical cyclones and typhoons according to the different human and social contexts

Owing to their frequency and potential devastating impact on coastal ecosystems and human communities in prone areas (Lam et al., 2009, 2011; Knutson et al., 2010; Rana et al., 2010), hurricanes, tropical cyclones and typhoons are particularly dangerous phenomena which are able to generate intense and widespread damage with territorial, agricultural and woodland repercussions (Conner, 1998; Boutet and Weishampel, 2003; Wang et al., 2010). Thus, they often give rise to dramatic social and economic consequences in developed countries and particularly in the most exposed urban contexts; at the same time, they represent “most hazardous events of many [...] socio-economic miseries” in the underdeveloped countries (Begum, Alam and Ali, 2013, p. 1), since their effects have long term repercussions and worsen already highly problematic situations.

Considerably different are the impact typologies caused according to the human and social contexts in which they break out.

In fact, in addition to the victims that unfortunately characterise both situations, in developed countries hurricanes, tropical cyclones and typhoons cause enormous damage, devastating cities and their surrounding zones, where considerable real estate, economic activities, commercial and imposing buildings or also monuments and museums are concentrated. The risk also concerns the possibility to involve sensitive capabilities, such as industries, power plants, oil platforms etc., generating environmental and ecosystem disasters on a large radius; then other kinds of sensitive areas can be affected, such as big hospitals, universities or colleges, resulting in impressive consequences with regard to social-healthcare or cultural-educational aspects.

Instead, in the underdeveloped countries the amount of infrastructural damage is considerably less relevant due to the very poor conditions and to the obvious minor potential

risk in terms of destructible built-up areas with dense arrangements of expensive buildings and sensitive structures of international relevance. Nevertheless, the impact is terrifying for the inhabitants because they see all their possessions being swept away, together with any hopes of improvement, in a humanitarian drama which initially catches the interest of the mass media but which within a very short space of time is often forgotten by the international attention. All this takes place in emergency conditions where the “imbalances in the imbalances” continue to increase and where local people and institutions do not have the capacity and strength to face the dramatic conditions alone, often accentuated by the spread of diseases connected to health and hygiene conditions and the transmission of oral-faecal diseases which become epidemics.

From some points of view, the “physiological resilience” of populations in the underdeveloped countries is generally lower, since they have objective problems in re-organising their lives, already scarred by widespread daily problems, and in coping with the trauma that has befallen them. It seems that they have “less to lose” and they are more accustomed to the suffering but the possibility of lifting themselves up in order to get out of the misery, basing themselves on their own resources and the support of local authorities, is very difficult. So they have “less to lose” in terms of personal real estate, property, great patrimonies, sensitive structures, but they have “more to lose” in the sense that they see everything that they own in order to survive disappear. On the other hand, people in the developed countries have a very strong psychological recoil due to the sudden loss of their comfort, commodities, high quality lifestyle and they fall into an abnormal and unusual condition, sometimes seeing the sacrifices of an entire lifetime being lost⁶.

⁶ Some reference studies on social resilience in the case of natural disasters are: Pelling, 2003, where many case studies, political measures and local governance, different disaster mitigation programmes, population disaster response network, the “disaster cycle” etc. are analysed; Cutter et al., 2008, who provide a place-based model for understanding community resilience and a list of indicators; Baker, 2009, where the factors enhancing

Therefore, space technologies and geotechnologies have a very important role in understanding some specific aspects of phenomena like hurricanes, tropical cyclones and typhoons and in elaborating a series of accurate measures and scenario analysis able to mitigate the possible consequences, damage and losses in both developed and underdeveloped countries.

4. Remote sensing for the study of hurricanes, tropical cyclones and typhoons. Input from literature

Remote sensing has a considerable “potential for documenting and aiding recovery from large and even small disaster areas. The timing of emergency response/post-disaster aerial surveys, extent of area covered, type of remote sensing technologies used, and expediency of data availability are some determinants of how well the remotely sensed data can be put to use” in order to give tangible benefits for the disaster response and the people rescue (Antalovich, 2011, p. 1185).

In this perspective, remote sensing and connected imagery and functionalities are “the main sources of information which allow monitoring the formation, development and movement” of hurricanes, tropical cyclones and typhoons, giving the possibility: “To monitor the formation and evolution of cloud systems; to find out the intensity of the cyclone; to study its movement and behavior; to identify and track of the cyclone formed in the Bay; to provide early warning that would be useful for disaster management and preparedness program” and necessary steps to face a potential disaster, as highlighted in the case of Cyclone MOHASEN, formed in the Bay of Bengal and whose peak along the Bangladesh coasts was recorded on May 15, 2013 (Begum, Nessa and Ali, 2013, pp. 95-96, 98). Remote sensing, numerical models and GIS applications, also with specific ex-

and/or constraining resilience are examined considering ten “paradoxes” which can have an important role. On collaborative resilience see: Goldstein, 2012. In the case of Hurricane Katrina some particular aspects related to resilience were for example investigated by: Metzl, 2009; Harville et al., 2010; Plyer et al., 2011.

tensions for spatial and detailed analysis, can be fundamental to hypothesize and estimate the maximum possible intensity of an event and its turbulence intensity and to make simulations regarding its evolution, providing important input in terms of civil protection as shown by: Durden, in 2010, as far as concerns Cyclone Monica, which occurred in April of 2006, having been formed to the east of Papua New Guinea and which fell along the northern coast of Australia; in 2011, Chan summarised the observations and measures made with sophisticated instruments for tropical cyclones affecting China’s south coasts and Hong Kong⁷. Furthermore, remote sensing is useful to evaluate the vulnerability of specific areas just prior to the events, to simulate the effects due to a widespread flooding and to provide an initial hazard assessment, as highlighted by Clinch et al., in 2012, with reference to Hurricane Irene that, on August 27, 2011, “made landfall near Cape Lookout and traveled north across Pamlico Sound and the Pamlico-Albemarle peninsula, creating a large surge on the sound side of the North Carolina Outer Banks” (p. 1). Moreover, the integration of remote sensing in GIS systems has shown its potentialities in order to conduct an “initial damage assessment analysis” for Atlantic City, New Jersey, USA, affected by Hurricane Sandy on October 29, 2012, also determining “the area of beach lost” and providing important input for emergencies phases, as for example the “major roads used for evacuation as well as the locations of first responders and schools within the city” (Heitshusen, 2012, p. 2).

Even if some problems can arise during similar atmospheric events, in the rapid and continuous acquisition of data and images with a good resolution⁸, the combined use of different

⁷ Further elements have been provided by Piñeros, Ritchie and Tyo, 2008, who have affirmed that the results of their research “show that the technique provides an objective measure of both the structure and the intensity of the tropical cyclone from early stages, through intensification, maturity, and dissipation” (p. 3574).

⁸ These problems are obviously intensified in the underdeveloped countries where the availability of instrumentations is minor and the humanitarian context, the social-economic aspects and the orga-

kinds of satellites, sensors and tools make it possible to increase the potential benefit which can be obtained and e.g.: the “microwave instruments provide a penetrating view below the upper level cirrus clouds” (Katsaros et al., 2002, p. 137)⁹; radar can reveal its added value during the night, through clouds and for the observation of internal waves, and Lidar (light detection and ranging) is very sensitive in recording the height of the terrain, obtaining altimetry information and data on coastline or urban changes resulting from erosion, including bathymetry and topography with high accuracy (Womble et al., 2006, p. 1; Klemas, 2009, p. 1273; 2012, p. 540). Thanks to radar interferometry it is possible to clearly show the most damaged areas by means of the comparison between images acquired before and after hurricanes, tropical cyclones and typhoons (<http://www.esa.int/ESA>).

An event which has undoubtedly given researchers of different sectors an opportunity to experiment and test innovative methodologies supported by remote sensing, also in an interdisciplinary approach, was Hurricane Katrina, which has its 10th anniversary in 2015. “Hurricane Katrina produced the largest peak storm surge observed in the Gulf of Mexico” (Turnipseed et al., 2007, p. 202). As far as concerns some peculiar aspects and data which characterised this devastating event, it is worthy of note that: “On August 29, 2005, Hurricane Katrina made landfall with sustained winds estimated at 125 mph, unprecedented storm surges approaching 30 feet and hurricane force winds extending 125 miles from its center. It resulted in over 1,300 lives lost, and caused major flooding and damage that spanned more than 200 miles along the Gulf Coast of the United States. [...] Hurricane Katrina caused significant damage to engineered infrastructure including levees, commercial and public buildings, roads and bridges, utility distribution systems for electric power and water, waste water collection facilities, and vital communication networks. Damage to critical infra-

nization of emergency planning denote many difficulties (REACH, 2014).

⁹ Regarding the satellite analysis of hurricanes and cyclones using advanced microwave instruments see also: Kidder et al., 2000; Zhu and Weng, 2013.

structure such as hospitals and communication systems crippled the affected communities” (Womble et al., 2006, p. iii). From a geophysics and meteorological point of view, another contribution underlined that it “originated as a tropical depression near the Bahamas on August 23, 2005, strengthened to a hurricane, and proceeded to make landfall on the southern tip of Florida. Passing across Florida, Katrina weakened to a tropical storm. However, the warm waters of the Gulf of Mexico allowed it to rapidly intensify to a Category 5 hurricane, with maximum sustained winds of 280 km/h and gusts of 346 km/h, generating 16.7-m waves. Subsequently, Katrina made landfall as a Category 3 hurricane near Buras, Louisiana, and once more near the Mississippi/Louisiana border with sustained winds of about 205 km/h” (Klemas, 2009, p. 1270). With regard to actual damage, above all in terms of economic loss and environmental impact, the literature remarked that “Katrina’s high winds and high storm surge combined to breach the levees protecting New Orleans, La., a city located below sea level, and flooded approximately 80 percent of the city. Katrina also caused major damage to the region’s oil and natural gas production and refining capabilities. On September 2, 2005, the Associated Press reported that Katrina had damaged 58 oil platforms, 30 of which were reported ‘lost,’ while 1 platform had been blown nearly 62 mi (100 km) from its original location” (Rykhus and Lu, 2007, p. 49). Additional details were provided by a further contribution which “estimated damages in excess of \$200 billion”, revealing Katrina as one of the most devastating and economically heavy hurricanes ever to shoot the United States and “enacted two supplementary appropriation bills totaling \$62.3 billion for emergency response and recovery needs”. Dramatic consequences were for example recorded about: “*Tourism (arts, entertainment, and recreation; accommodation and food service); Port operations (mining; transportation and warehousing); Educational services*” (Dolfman, Wasser and Bergman, 2007, pp. 3-4). Moreover, an initial approximate “assessment by the Mississippi Forestry Commission estimated that over \$1 billion in raw wood material was downed by the storm, with county-level damage percentages ranging from 50 percent to 60 percent across

Mississippi's three coastal counties" (Collins et al., 2010, p. 225).

A relevant study, concerning the damage detection for Hurricane Katrina using an integration of different remote sensing data with satellite (*low-, moderate-, high-resolution*) and aerial imagery, was conducted by Womble et al. in 2006. "In the aftermath of Hurricane Katrina, remote sensing data from satellite and airborne platforms were collected rapidly and made available to support post-disaster situation assessment and response activities in Mississippi and Louisiana. While weather satellites provided constant monitoring of the storm track, given the limited ground access due to surge inundation and flooding, remote sensing imagery constituted one of the first available sources of information on damage conditions" (p. 9). The *low-resolution* satellite imagery was for example used to show: "pre-hurricane conditions in the rivers of southeast Mississippi and southwest Alabama on August 27, 2005 and post-hurricane flood levels on August 30, 2005, one day after Hurricane Katrina's landfall in Louisiana" (p. 17); "the flooding conditions in the City of New Orleans and in the land areas between Lake Pontchartrain and Lake Borgne" (p. 15). The *moderate-resolution* satellite imagery was for example used to reveal "flooding extent in New Orleans on August 30, 2005" also through the comparison with the situation of some days before (p. 19). Moreover this kind of documentation was analysed to observe "the progression of rising and receding flood waters" in New Orleans (p. 20) on the basis of images recorded on September 6 and 8, 2005. The *high-resolution* satellite imagery made it possible to highlight information regarding individual buildings, creating the basis for a very useful and detailed framework of the recorded damage. In this perspective of collection and dynamic archiving of data and information, in order to promote reconnaissance and emergency planning, the integration between (*high-resolution*) satellite imagery and aerial images clearly show its importance and utility in assessing damage to buildings, bridges and roads and other infrastructures, in identifying the most stricken and needy areas, estimating socio-economic

effects of the disaster and in better predisposing and organising medical treatment and hygiene services.

Another notable study was edited by Farris et al., in 2007, who published the results of a multidisciplinary piece of research that involved a large panel of experts in geography, geology, geospatial information, biology etc. to make a structured framework of knowledge regarding hurricanes, with particular attention to the most relevant ones to be recently recorded and above all Katrina. For example, Rykhus and Lu used a multiple-database approach that integrated and combined many remotely sensed data of different kinds "to map Hurricane Katrina-induced flooding and to identify offshore oil slicks", because similar elaborations can provide fundamental "information to emergency managers for directing flood-relief efforts and the clean-up of polluted waters" (2007, p. 49). At the same time, Gesch used remote sensing to produce topography based representations able to provide – thanks to the re-elaboration of imagery with considerable spatial details and vertical accuracy of elevation measurements – rough estimates of the inundation of New Orleans, caused by Hurricane Katrina. The results obtained made it possible to put forward considerations on the necessity regarding the future planning reconstruction of buildings and infrastructures, with special mitigation measures against similar events. Moreover, some inputs were provided concerning the importance of considering the inundation history of an area and its general condition in order to correct and modify the modelling scenarios on the basis of the actual local situation (2007, pp. 53, 56). Smith and Rowland also processed and analysed satellite images and data from various sensors to measure and evaluate the extent of the flooding caused in New Orleans by Hurricane Katrina, following the definition of specific polygons of inundated areas. Thus, the numerous and continuous satellite acquisitions, the use of GIS techniques and the availability of high-resolution digital elevation models (DEM), enabled them to monitor "the floodwater volume and extend through time" (2007, p. 57).

A couple of years later, Gesch published an interesting paper which considered both Hurricane Katrina and Hurricane Rita, producing a

series of highly explicative elaborations. “Surveyed high-water marks were used to generate a maximum storm-surge surface for Hurricane Katrina extending from eastern Louisiana to Mobile Bay, Alabama. The interpolated surface was intersected with high-resolution lidar elevation data covering the study area to produce a highly detailed digital storm-surge inundation map. The storm-surge dataset and related data are available for display and query in a Web-based viewer application¹⁰. A unique water-level dataset from a network of portable pressure sensors deployed in the days just prior to Hurricane Rita’s landfall captured the hurricane’s storm surge. The recorded sensor data provided water-level measurements with a very high temporal resolution at surveyed point locations. The resulting dataset was used to generate a time series of storm-surge surfaces that documents the surge dynamics in a new, spatially explicit way. The temporal information contained in the multiple storm-surge surfaces can be visualized in a number of ways to portray how the surge interacted with and was affected by land surface features” (2009, p. 1).

In the same year, other considerations regarding the synergic use of different images, sensors and tools to deal with disasters and evaluate the impact of a dramatic event, like the one produced by Hurricane Katrina, were illustrated by Klemas (2009). In particular, he affirmed that: “Satellite images and hurricane hunter planes were used to track hurricane Katrina, with modelers predicting accurately its path, strength, surge level, and landfall location. Shore-based radars were used to confirm the data as the hurricane approached land. Medium- and high-resolution satellite sensors, helicopters, and aircraft were employed to assess damage to the city [New Orleans and near areas], including transportation, power, and communication infrastructures, and to adjacent wetlands and other coastal ecosystems” (p. 1264)¹¹.

Both Womble et al. (2006) and Klemas (2009) have also underlined the importance of systems such as Google Earth which can be very

useful in terms of information sharing and can produce applications and visualizations that show, in a very short time, areas with high levels of damage and the possible routes to reach these neuralgic zones. For example, Google Earth (Klemas, 2009, p. 1273): “preloaded on laptops to survey and map the destruction and flooding”; “delivered a vivid three-dimensional model of the city [New Orleans] and its surroundings, providing a high-performance visualization interface” which became essential during the emergency and recovery phases. At the same time: “The Internet-based Google Earth application likewise provided a publicly-accessible means for distributing VIEWSTM ground reconnaissance information collected by the [...] advanced technology field teams. Within the Google Earth framework, geographically referenced VIEWSTM field reconnaissance data are readily integrated with remote sensing imagery” (Womble et al., 2006, p. 119). In this way, specific image sets were produced by using the functionalities of Google Earth, combined with the field survey data for example recorded with GPS, to show wind-pressure, storm surge and flooding damage in various zones, on different geographical scales, and to have easily accessible data via the online applications.

Similar geobrowsers therefore became strategic tools for rescuers and the inhabitants of heavily damaged areas and the easiness of these image visualizers to interface with other geotechnologies, like GIS software, enabled them to continuously elaborate and share updated layers with detailed information useful for social, sanitary, emergency purposes (Favretto, 2009, pp. 18-19).

With reference to the aspects related to land use and vegetation loss, in 2010 Wang et al. validated an approach based on remote satellite sensing and statistical analysis for the estimation and quantification of the forest damage severity caused by Hurricane Katrina. Through a study of land cover type, the application of change detection methods and the identification of proper damage indicators, they produced different maps of forest damage levels.

One year later, Lam et al. (2011) – starting from the assumption that an exhaustive as-

¹⁰ See http://topotools.cr.usgs.gov/Katrina_viewer/.

¹¹ For further considerations see Collins et al., 2010.

assessment of the effects caused by hurricanes on coastal ecosystems would be useful to promote specific policies finalized at mitigating the potentially devastating impacts of future events – compared “the land cover change around Weeks Bay, Alabama, USA following landfalls of Hurricanes Ivan and Katrina (September 16, 2004 and August 29, 2005)” (p. 1707). Analysing different satellite imagery concerning the pre- and post- hurricanes arrival, they evaluated the variations recorded in terms of damage (for example widespread defoliation of trees and invasion of specific areas) and changes, with relative rates of loss and gain, in the classes of land cover.

Thus, in terms of scientific research, each hurricane, tropical cyclone and typhoon should represent a “test bench” from which to obtain precious study elements, essential to learn a concrete lesson and thanks to which reduce the potential impact of successive events. That is to say that they should become the ‘unfortunate’ opportunity to record the actual developments in terms of scientific knowledge and to avoid other similar tragedies occurring without having decreased the entity of the damage proportionally to the asserted possibilities.

5. For a didactical reflection

For the relevance of social and economic effects, the amount of territorial modifications which are recorded and for the frequency of occurrence, the study of hurricanes (and natural disasters), supported by remote sensing and geotechnologies, takes on considerable importance also with regard to didactics and education. As affirmed by Morin in 2005 (pp. 367-368): “Remotely sensed images provide emergency response officials and scientists with a unique perspective for assessing damage and targeting relief. These images also offer educators a unique, teachable moment for the classroom”. In fact, a dramatic event such as Hurricane Katrina can make school lessons and, particularly, Geography and Earth science “relevant in a way that a daily lecture cannot”. A critical interpretation of similar images, above all in a well organised cycle of lessons also focussed on the use of GIS, Google Earth, Bing

and other geobrowsers, can give the students a more sensitive and conscious viewpoint on the interaction between geophysical aspects and human society.

In these cases, the use of satellite and aerial images, combined with geobrowsers or integrated in a GIS platform, can make the lesson highly educational, arousing attention, interest and emotion, in a participatory atmosphere where students can interpret and elaborate images in teamwork and discuss with teachers the causes, the extent of the consequences and the damage, the possible planning of emergency measures, gaining awareness of the weak points of the urban contexts and highly inhabited coastal areas etc.

Moreover, the mixing of possibilities provided by geomatic methods of change detection and GIS applications for evaluating the modifications recorded in the land use classes can give considerable didactic and research stimuli, opening up new possibilities in terms of practical exercises, laboratory and assessment tests.

Therefore, geotechnologies become a privileged tool to connect theoretical content with practical aspects, creating an opportunity for personal hypothesis, reflecting on possible guidelines to support decision-making, in the awareness of the importance of an interdisciplinary approach assisted by geography and enriched by geospatial technologies. In this way, geotechnologies make it possible to move towards a dynamic, participative and cooperative learning approach, finalised at providing geographic competence and computer skills to better understand and analyse relevant problems which concern both physical and anthropic spheres, bringing about a series of impacts and social-economic consequences in the long term.

6. Hurricane Katrina

Katrina was an extraordinarily powerful hurricane, estimated to be the costliest and one of the five deadliest that ever struck the United States of America¹².

Similarly to many of the hurricanes formed in the Atlantic region, the genesis of Katrina involved the interaction of a tropical perturbation originated over Africa traveling westward. This atmospheric wave, over the Bahamas, met with weather conditions residual of a previous tropical depression (td10) (Figure 7) and the progressive weakening of an upper tropospheric mid-latitude deep trough (that is to say an extensive intrusion of relatively colder air) and its corresponding vertical wind shear, thereby becoming Tropical Depression 12 (Figure 8). Both these circumstances favour the formation of a tropical cyclone.

Based on wind data measured at flight level by reconnaissance aircrafts, the cyclone became Katrina, the 11th tropical storm of the 2005 Atlantic hurricane season, at 12.00 UTC on 24 August, when it was centered over the central Bahamas about 120 km (65 nautical miles) east-south-east of Nassau. Initially the storm moved north-westward (Figure 9). However, as it developed an inner core and evolved into a deeper cyclone on 24 August, it came under the influence of a strengthening middle to upper tropospheric high pressure ridge over the northern Gulf of Mexico and southern USA. This ridge turned Katrina westward on 25 August toward southern Florida. Katrina generated a notable burst of deep convection over the low-level centre during the afternoon of 25 August while it was located over the north-western Bahamas. Other strengthening ensued and Katrina reached hurricane status at near 21.00 UTC on 25 August, less than two hours before its centre made landfall on the south-eastern coast of Florida (Figure 10).

This interaction with the land was too shortly lived to cause a substantial weakening of Katrina. As a matter of fact, the formation of the eye of the hurricane was first detected by the Miami National Weather Service (NWS) WSR-88D Doppler radar just prior to landfall on the south-eastern Florida coast (Figure 11).

¹² For this paragraph, the contribution written by Knabb, Rhome and Brown, 2011, has represented the main reference paper and some its excerpts are here reported and analysed.

As it crossed southern Florida the convective pattern of Katrina was rather asymmetric, having the strongest winds and heaviest rains south and east of the center in Miami-Dade County (red area in Figure 11). Once back over water, Katrina quickly regained the hurricane status at 06.00 UTC on 26 August with maximum sustained winds of 120 km/h (65 knots). Situated beneath a very large upper-level anticyclone that dominated the entire Gulf of Mexico by 26 August, resulting in very weak wind shear and efficient upper-level outflow, Katrina embarked upon two periods of rapid intensification between 26 and 28 August.

The first period involved an increase in the maximum sustained winds of up to almost 175 km/h (95 kt) in the 24-h period ending at 06.00 UTC on 27 August. An eye became clearly evident in infrared satellite imagery early on 27 August, and Katrina became a Category 3 hurricane with 185 km/h (100 kt) winds at 12.00 UTC that morning at about 675 km (365 n mi) SE of the mouth of the Mississippi River.

Katrina nearly doubled in size on 27 August, and by the end of that day tropical storm-force winds extended up to about 260 km (140 n mi) from its centre. Unfortunately for the USA, the large scale atmospheric circulation that originally kept Katrina on a west-south-westward track evolved unfavourably and Katrina turned north-westward on 28 August (Figure 12) after having produced tropical storm-force winds and heavy rainfall over portions of western Cuba on the 27th. The new eyewall contracted into a sharply-defined ring by 00.00 UTC of 28 August, and a second, more rapid intensification then occurred. Katrina strengthened from a low-end Category 3 hurricane to a Category 5 one in less than 12 hours, reaching an intensity of 270 km/h (145 kt) by 12.00 UTC on 28 August. Katrina recorded its peak intensity of almost 280 km/h (150 kt) at 18.00 UTC on 28 August about 315 km (170 n mi) southeast of the mouth of the Mississippi River. Figure 8 (right) shows a satellite image of the fully developed hurricane Katrina acquired in the Visible spectral band by the NOAA geostationary meteorological satellite GOES-12. The hurricane minimum central pressure dropped that afternoon to 902 mb. Figure 13 gives an idea about the size of Katrina with respect to the geography of the Gulf of Mexico and southern USA.

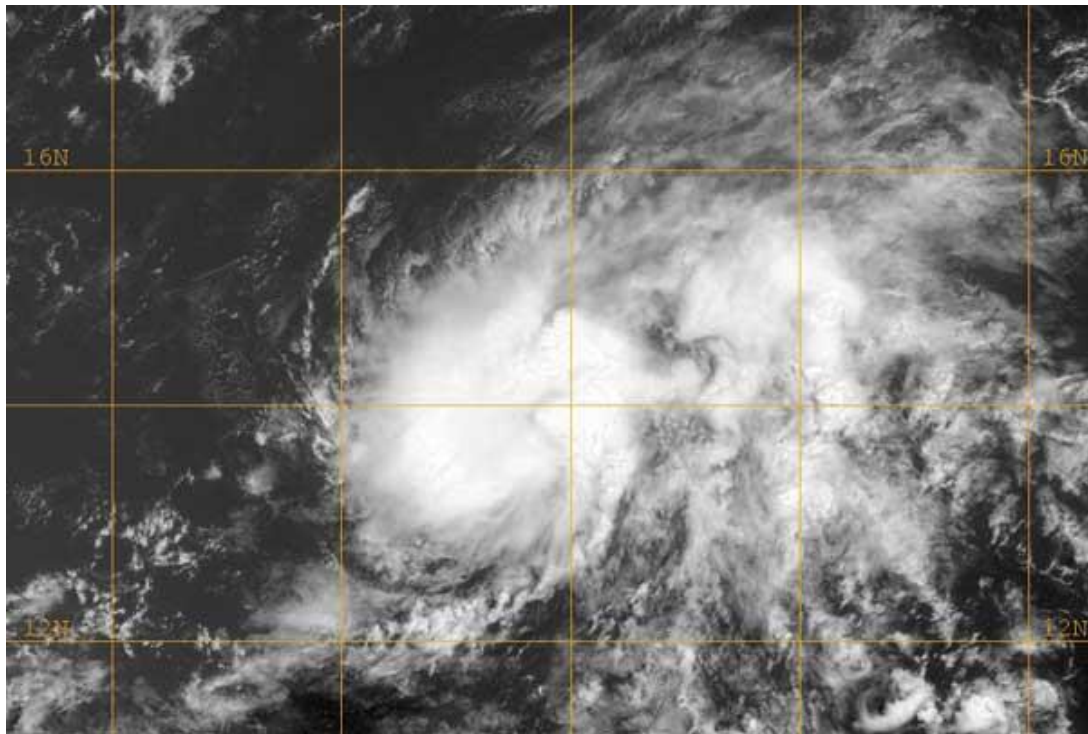


Figure 7. Satellite image of Tropical Depression 10 in the eastern Atlantic Ocean on 13 August, 2005. Courtesy of the US Naval Research Laboratory.



Figure 8. Left: the Tropical Depression 12 over Bahamas on 23 August 2005. Right: the Category 5 hurricane Katrina on 28 August 2005. Courtesy of NOAA.

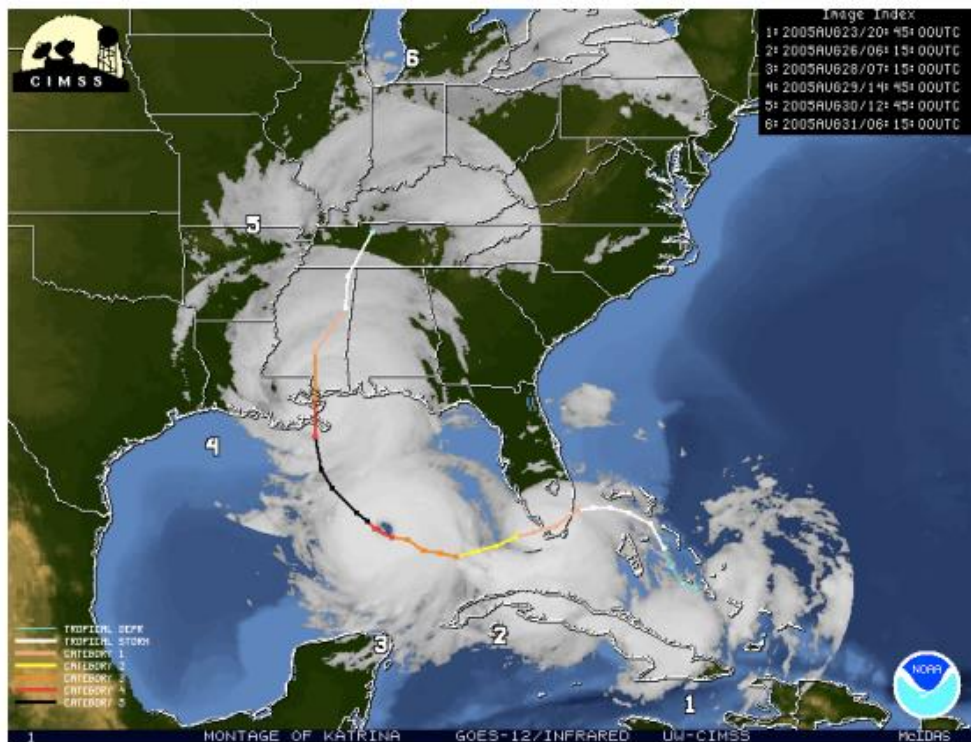


Figure 9. Katrina track and intensity. Courtesy of NOAA.

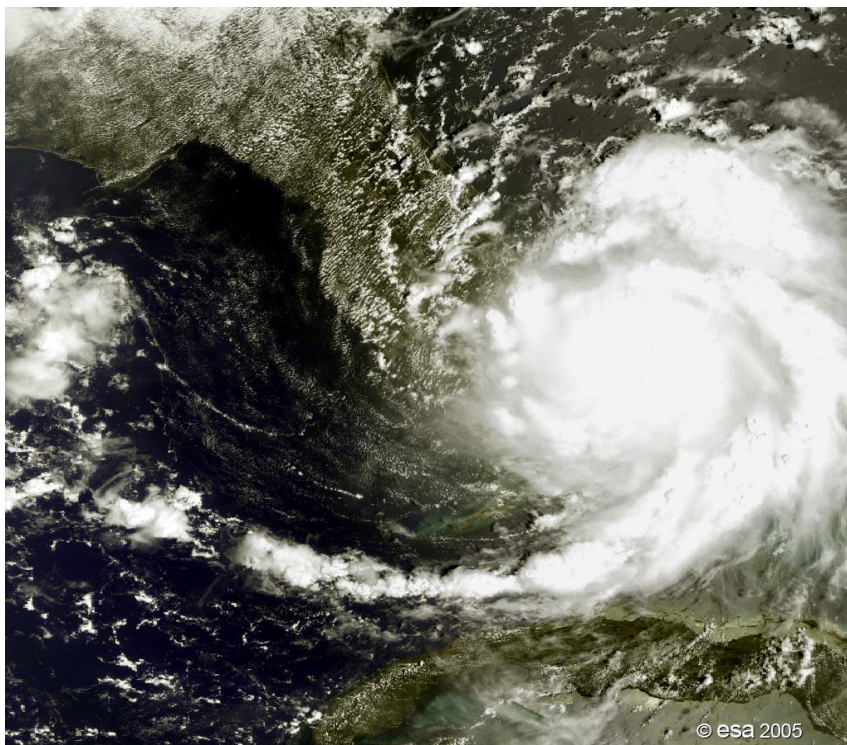


Figure 10. Hurricane Katrina as observed in the Visible spectral bands by the MERIS instrument of the Envisat satellite in Reduced Resolution mode, off southern Florida on 25 August 2005, when it was still Category 1 (Saffir-Simpson scale measuring hurricane intensity). The storm provoked notable damage after landfall, mostly due to heavy rainfall. Courtesy of ESA.

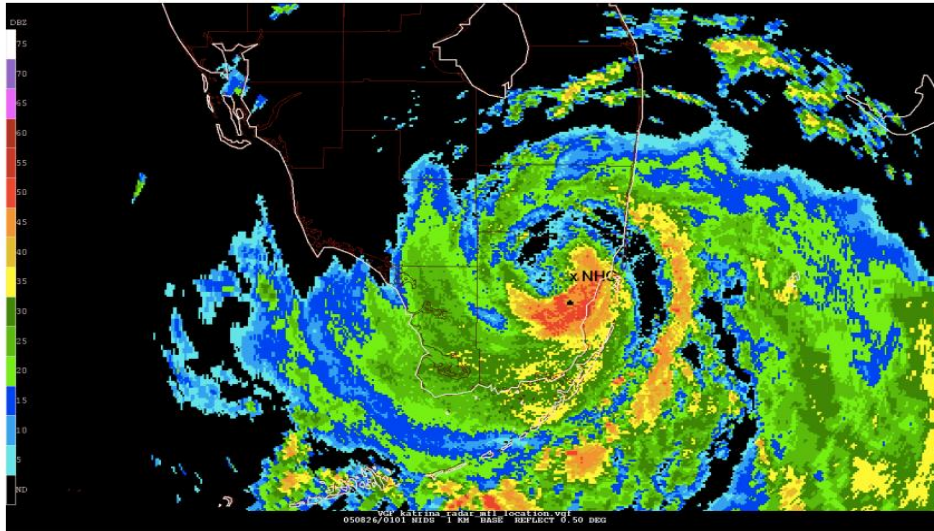


Figure 11. Radar reflectivity image at 01.00 UTC on 26 August 2005, as the center of Hurricane Katrina passed over Miami (Florida) and near the NWS Miami Weather Forecast Office/National Hurricane Center (located where specified by the “x”-“NHC”). Courtesy of NOAA.

Although tropical cyclones of category 5 strength are rarely sustained for any length of time (due to internal dynamics), Katrina continued to be a strong category 4 strength hurricane despite the entrainment of dryer air and an opening of the eyewall to the south and southwest before landfall on the morning of the 29th. Characteristics of the hurricane at landfall are shown in Figures 14 and 15.



Figure 12. Eyewall of Hurricane Katrina taken on August 28, 2005, as seen from a NOAA P-3 hurricane hunter aircraft before the storm made landfall on the USA Gulf Coast. Courtesy of NOAA.



Figure 13. Image of the Hurricane Katrina acquired in the Visible spectral band by the geostationary meteorological satellite GOES-12 on 28 August 2005 at 21.15 UTC. Courtesy of NOAA.

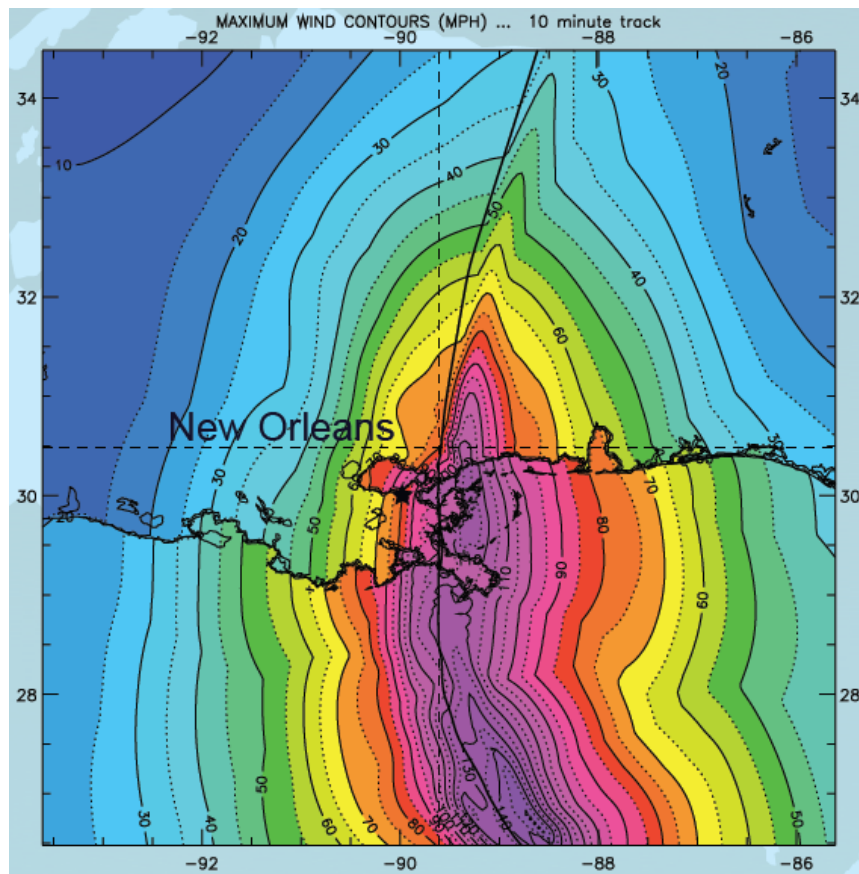


Figure 14. Landfall wind speeds at Grand Isle in Louisiana were about 205 km/h (110 kt) (strong category 3 intensity), with a central pressure of 920mb. Courtesy of NOAA – National Hurricane Center.



Figure 15. Hurricane Katrina at landfall over the Louisiana coast on 28 August 2005. Courtesy of NOAA.

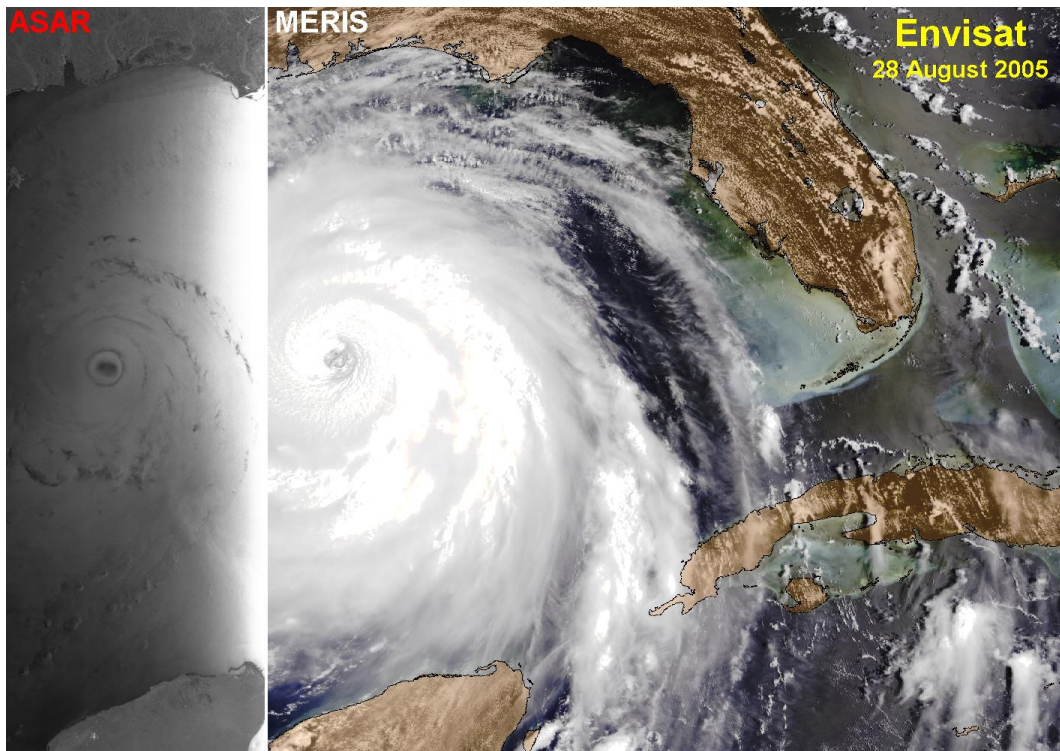


Figure 16. “Two separate views of Hurricane Katrina acquired on 28 August 2005 from instruments aboard Envisat. The ASAR Wide Swath mode radar image of the sea surface shows how Katrina’s wind fields are rippling the ocean. Beside it is the MERIS Reduced Resolution mode optical images showing characteristic swirling cloud patterns around the central eye, with the eyewalls visible” (http://www.esa.int/spaceinimages/Images/2005/08/Envisat_views_of_Hurricane_Katrina). Courtesy of ESA.



Figure 17. Flooding in the Metairie area of New Orleans visible in a radar image acquired on 31 August 2005 by the ASAR instrument of the Envisat satellite, following Hurricane Katrina. Courtesy of ESA.

Figure 16 shows how remote sensing techniques provide a major help in monitoring hurricanes by acquiring data detected in different spectral bands and taking advantage of their characteristic spectral signatures. In these images, on the right hand side Katrina is monitored by the superspectral MERIS instrument in the Visible spectral bands, therefore in a way similar to the viewing of a human eye, hence showing characteristic swirling cloud patterns around the central eye, with the eyewalls visible. On the left hand side, instead, the hurricane is imaged by ASAR, the Synthetic Aperture Radar aboard the ESA Envisat satellite, in the microwave C-band of the electromagnetic spectrum, that is to say through e.m. pulses at a wavelength of 10 cm: that implies that the radar energy backscattered to the ASAR by the target “illuminated” by the radar pulses provides information, among other, about the surface roughness, the electric characteristics of the target and the size of the encountered cloud and rain droplets, if any. In this ASAR image, the central dark area of about 40x30 km² indicates a smoother sea surface, due to the lack of winds at the central extreme low pressure, surrounded by a circular whitish very rough sea surface (high radar backscatter) due to strong eyewall winds, which includes a dark ring probably generated by the very strong radar energy attenuation caused by the big thunderstorm heavy rain droplets.

Though wind damage was significant, the legacy of Katrina will be the horrific storm surge which accompanied the hurricane. Such massive storm surge produced by Katrina, even though it had weakened from Category 5 intensity, the previous day in Louisiana, it can be generally explained by the huge size of the storm: on 29 August Katrina had an extent of (about 45-55 km, 25-30 n mi) radius of maximum winds and a very wide swath of hurricane force winds that extended at least 140 km (75 n mi) to the east from the centre. Also, Katrina had already generated large northward-propagating swells, leading to substantial wave setup along the northern Gulf coast, when it was at Category 4 and 5 strength) during the 24 hours or so before landfall.

A surge of 8-9 m was estimated along the western Mississippi (MS) coast across a path of about 30 km, tapering to a height of 6-7 m along

the eastern MS coast. The maximum high water mark observation was 8.5 m at Pass Christian, MS. Alabama’s coast experienced surges ranging from as high as 3 m in the east to 5 m in the west. Surges in eastern Louisiana generally ranged from 3 to 5 m. The 920 mb central pressure at landfall and the shallow offshore waters also contributed to the extreme storm surge.

Figure 17 shows flooding in the Metairie area of New Orleans which is visible in a radar image acquired on 31 August 2005 by the ASAR instrument of the Envisat satellite, following Hurricane Katrina. “Most of New Orleans lies below sea level and is protected by canals, walls, dykes and pumps. The areas of the city which were flooded (bluish areas) by as much as six metres of water after two levees or dykes burst on 30 August on canals leading to Lake Pontchartrain. Lake waters continued to rise on 30 and 31 August and water poured into the city as pumps had failed. The circular area of the New Orleans Superdome, where thousands of trapped residents sheltered during the worst of the hurricane, is barely visible to the northwest of the double span of the Greater New Orleans Bridge, across the Mississippi from the Algiers Point Revetment at the first bend of the river at the right edge of the image. Water was waist-high in the area when this image was acquired. The area west of City Park, the dark area at centre image just east of the I-10 Bridge bordering on the Orleans Outfall Canal, also appears to be heavily flooded. Both airports were also under water”¹³.

7. Typhoon Haiyan

Typhoon Haiyan occurred in November 2013 and struck the central Philippines causing devastation due to its exceptionally strong winds and storm surge, so that it is also known as Super-Typhoon Haiyan. Sustained winds averaged over 1-minute were estimated to be near 315 km/h at landfall and the central pressure estimated as 895 mb leaving Typhoon Haiyan likely to be the strongest tropical cyclone (in terms of wind speed) to make landfall on record.

¹³ See https://earth.esa.int/web/earth-watching/natural-disasters/cyclones/cyclone-events/-/asset_publisher/4Llz/content/hurricane-katrina-florida-august-2005.

On 2 November, a broad low-pressure area was located about 425 kilometers (265 miles) east-southeast of Pohnpei, in the Federated States of Micronesia.

This system, which developed possibly in association with an Equatorial Rossby wave (a westward moving atmospheric wave near the Equator that can trigger convergence in the lower levels of the atmosphere and, moving through a region, favour tropical cyclogenesis), was first classified as a tropical depression when it was located near 6° N on 3 November.

On 4 November, Haiyan first reached tropical cyclone strength, defined as winds greater than 63 km/h, and then it continued to gain force. Subsequent intensification resulted in Haiyan being upgraded to tropical storm and assigned the name Haiyan (“petrel”) at 00.00 UTC on 4 November. Tracking generally westward along the southern periphery of a subtropical high pressure system, rapid intensification was recorded by 5 November, as a central dense overcast with an embedded eye began developing. Following this, Haiyan was reclassified as a typhoon later that day. By 6 November, as it approached the area under the Philippine Atmospheric, Geophysical and Astronomical Services Administration gave local name “Yolanda” to the storm. Intensification slowed somewhat during the day, though the storm was considered as having attained Category 5-equivalent super typhoon status on the Saffir-Simpson hurricane wind scale at around 12.00 UTC¹⁴. The westward movement of Haiyan accelerated: in the early morning of 7 November it was located still east of the Philippine islands (Figure 18), but it had already reached them in the evening of the same day (Figures 19-22).

As a typhoon, the winds around Haiyan reached a maximum sustained wind strength of 232 km/h and a maximum intensity (lowest barometric pressure in the storm eye) of 895 mbar (hPa) at 20.40 on 7 November. Unofficial estimates suggest that Haiyan attained one-minute sustained winds of 315 km/h (195 mph) and gusts of up to 378 km/h (235 mph), making it the most powerful storm ever recorded to strike land.

¹⁴ For further details see Odow, 2015.

As customary, interaction with land produced small degradation of the storm’s structure, though it remained an extraordinarily powerful one when it struck the municipality of Tolosa, Leyte, at around 22.30 UTC on the same day (Figures 21 and 22).

“When Super Typhoon Haiyan, one of the most powerful storms ever recorded on Earth, struck the Philippines on 8 November 2013, it tore a wide swath of destruction across large parts of this island nation”. Tacloban City was struck by the northern eyewall, the most powerful part of the storm. “To assist in the disaster response efforts, scientists at NASA’s Jet Propulsion Laboratory, Pasadena, Calif., in collaboration with the Italian Space Agency, generated an image of the storm’s hardest-hit regions, depicting its destruction (Figure 23). The 40-by-50 kilometer damage proxy map, which covers a region near Tacloban City, where the massive storm made landfall, was processed by JPL’s Advanced Rapid Imaging and Analysis (ARIA) team using X-band interferometric synthetic aperture radar data from the Italian Space Agency’s COSMO-SkyMed satellite constellation. The technique uses a prototype algorithm to rapidly detect surface changes caused by natural or human-produced damage. The assessment technique is most sensitive to destruction of the built environment. When the radar images areas with little to no destruction, its image pixels are transparent. Increased opacity of the radar image pixels reflects damage, with areas in red reflecting the heaviest damage to cities and towns in the storm’s path. The time span of the data for the change is 19 August-11 November 2013. Each pixel in the damage proxy map is about 30 meters across”¹⁵.

The typhoon made four additional landfalls as it traversed the Visayas, Daanbantayan, Bantayan Island, Concepcion, and Busuanga Island.

¹⁵ See <https://www.nasa.gov/content/goddard/haiyan-northwestern-pacific-ocean/#.VXmqovntmko>. See also <http://photojournal.jpl.nasa.gov/catalog/PIA17687> and <http://aria.jpl.nasa.gov/>.

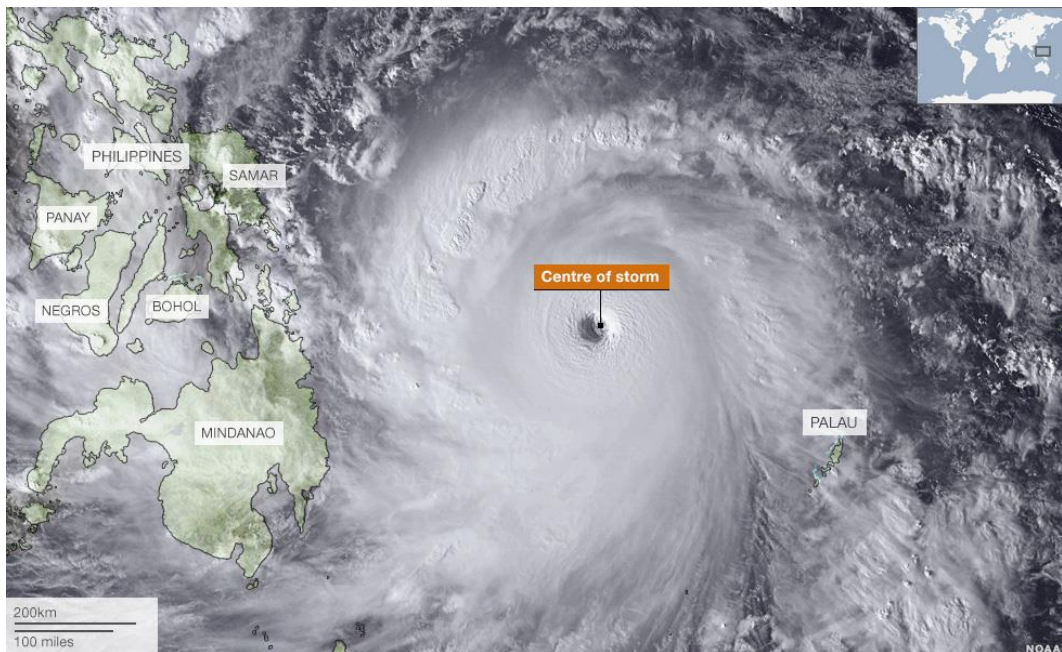


Figure 18. Typhoon Haiyan observed in the Visible spectral band of MTSAT geostationary satellite in the early morning of 7 November 2013. Geography and islands' names are added. Courtesy of BBC/NOAA/JMA.

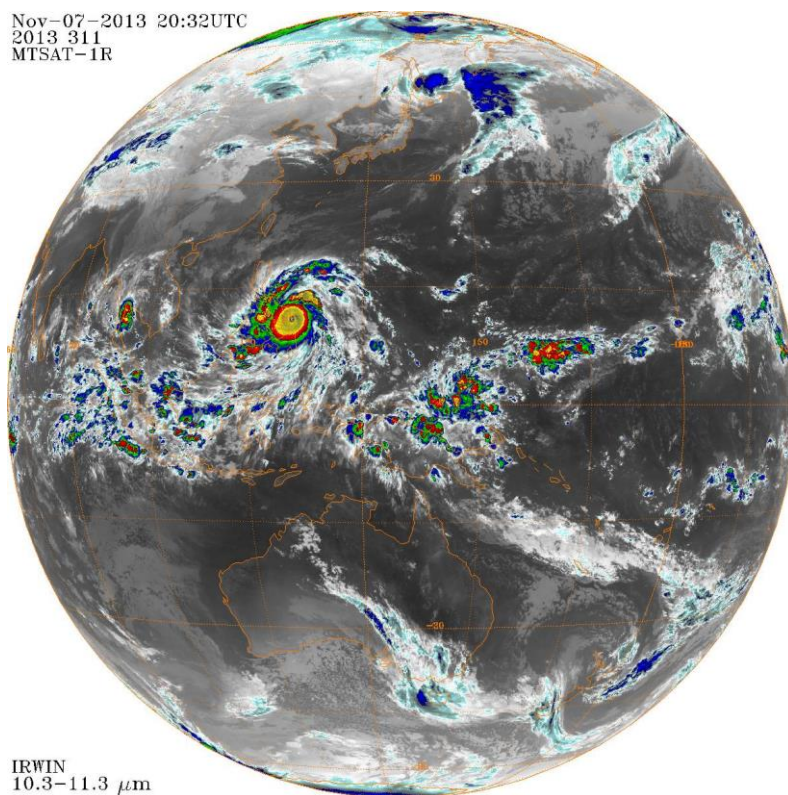


Figure 19. Earth full-disk image acquired in the Thermal Infrared spectral band by the Japanese MTSAT-1R geostationary satellite at 20.32 UTC on 7 November 2013. Very cold Cloud Top Temperatures (i.e. very high cloud tops) are visualized in a colour scale, from cyan ($-40\text{ }^{\circ}\text{C}$) to yellow ($-80\text{ }^{\circ}\text{C}$) and dark-yellow ($<-80\text{ }^{\circ}\text{C}$). Courtesy of JMA and NOAA.

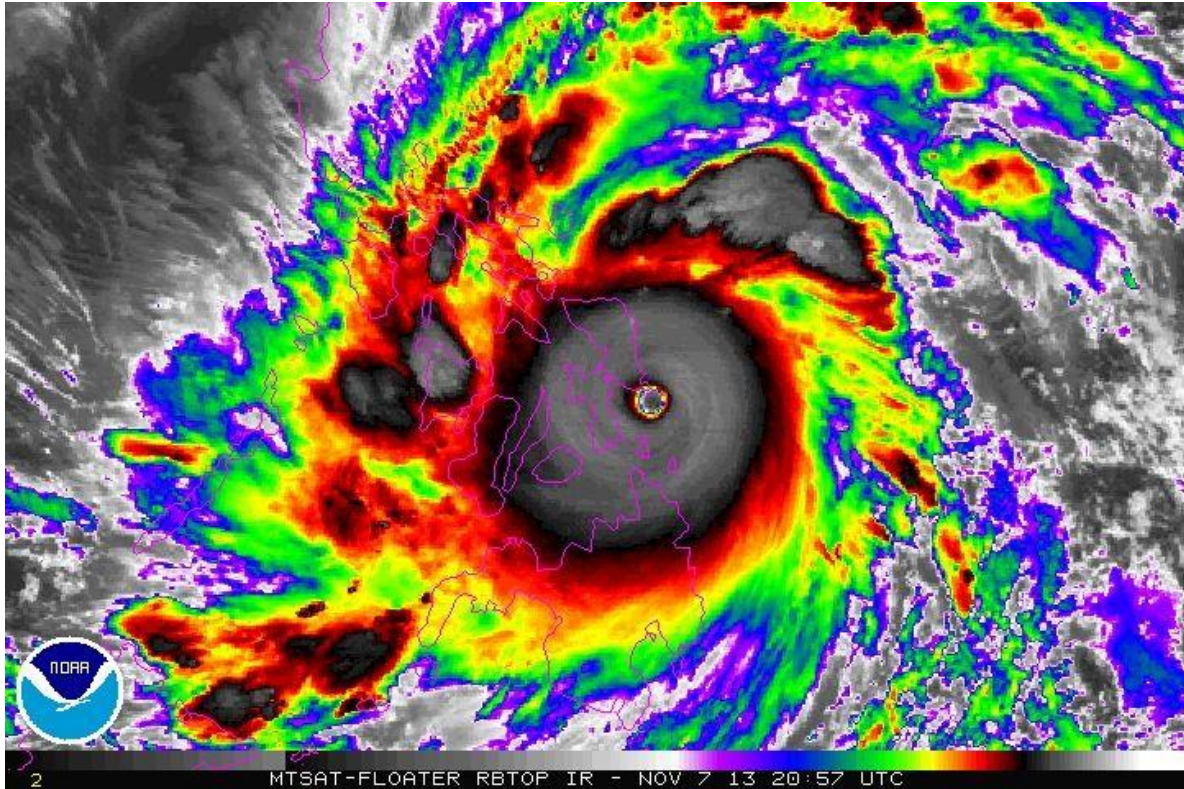


Figure 20. Typhoon Haiyan observed in the Thermal Infrared spectral band by the Japanese MTSAT-1R geostationary at 20.57 UTC on 7 November 2013. Courtesy of JMA and NOAA.



Figure 21. Same as Figure 18, but acquired at 22.30 UTC of the same day. Courtesy of NOAA.

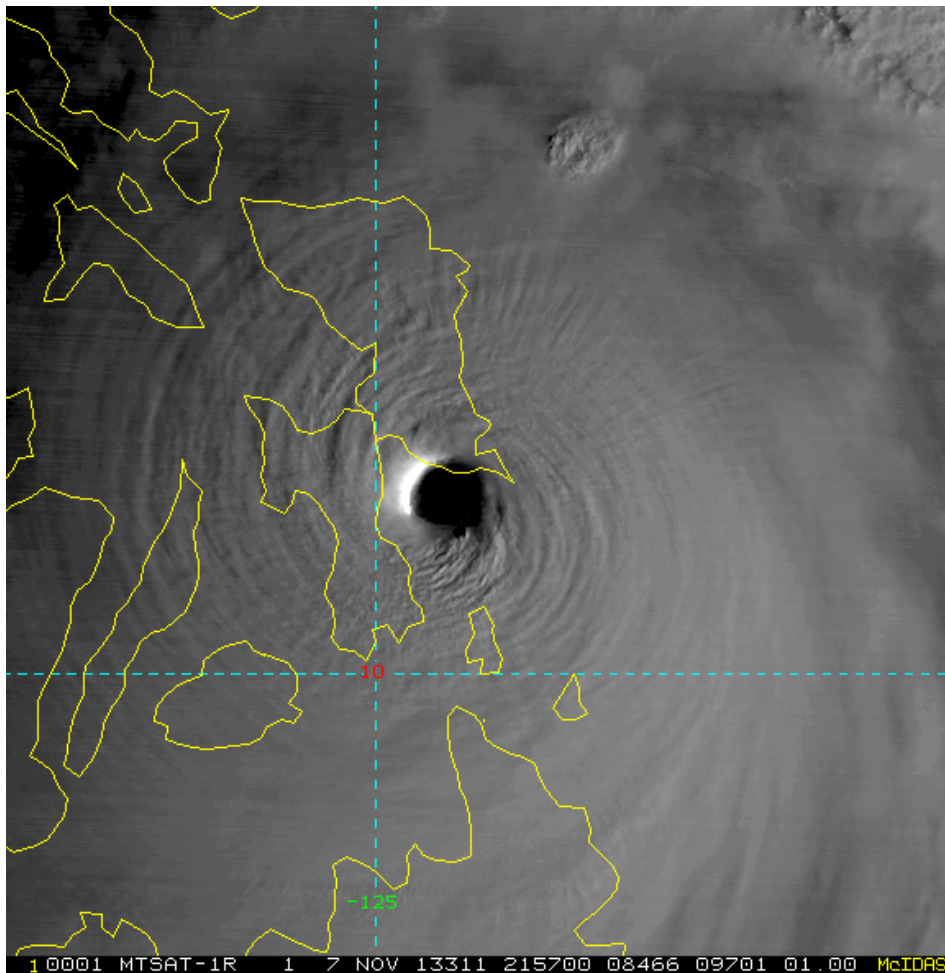


Figure 22. The eye of typhoon Haiyan imaged in the Visible spectral band by the MTSAT-1R geostationary EO satellite on 7 November 2013, just before its landfall on the island of Leyte at around 22.15 UTC. Courtesy of JMA and NOAA.

A weakened Haiyan, with its core disrupted by interaction with the Philippines, emerged over the south China Sea late on 8 November. Convection was diminished around the low-level circulation centre, despite overall remaining tightly wrapped although some cool, stable air flowed in from the west.

Continuing across the south China Sea, Haiyan turned more north-westerly late on 9 November and through 10 November (Figures 24 and 25), as it moved around the southwestern edge of the subtropical ridge previously steering it westward.

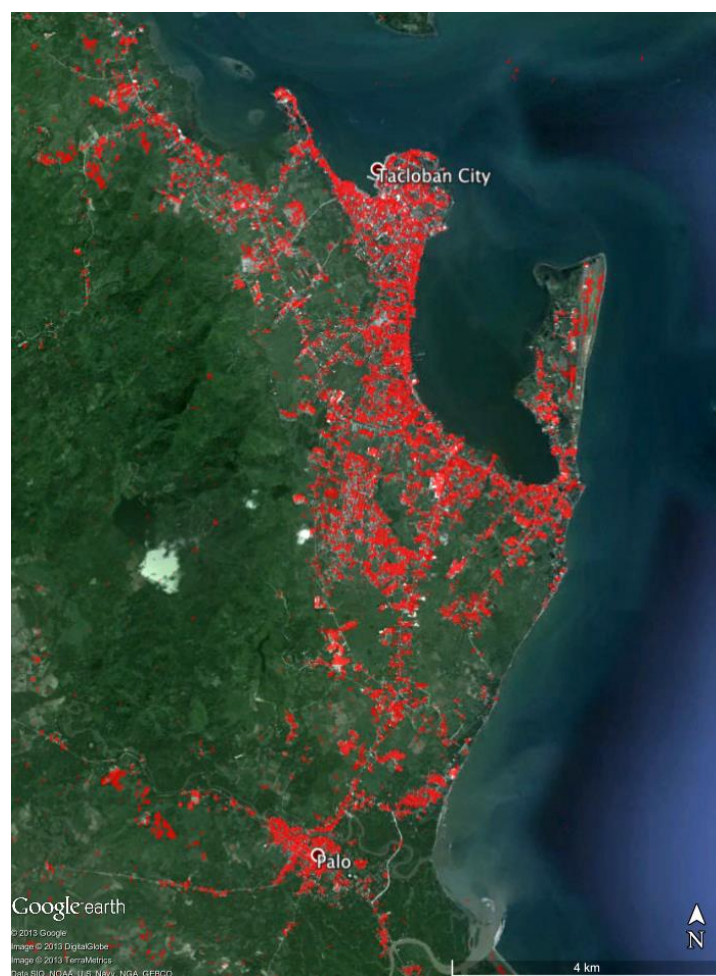


Figure 23. A radar composite showing in RED the areas most devastated by the typhoon Haiyan. Courtesy of ASI/NASA/JPL-Caltech.



Figure 24. NASA astronaut Karen Nyberg took this photo of Typhoon Haiyan from the International Space Station on 9 November 2013, a day after it passed over the Philippines. Courtesy of NASA.



Figure 25. “The Moderate Resolution Imaging Spectroradiometer (MODIS) on NASA’s Terra satellite captured this image of Typhoon Haiyan approaching Vietnam on November 10, 2013. The storm was tracking northwest and slowly weakening prior to landfall in northern Vietnam on Sunday evening (Monday morning, local time). As of early Sunday morning, the storm had maximum sustained winds of about 90 miles (145 kilometers) per hour, the equivalent of a category 1 storm” (<http://visibleearth.nasa.gov/view.php?id=82372>). Courtesy of NASA EO Observatory.

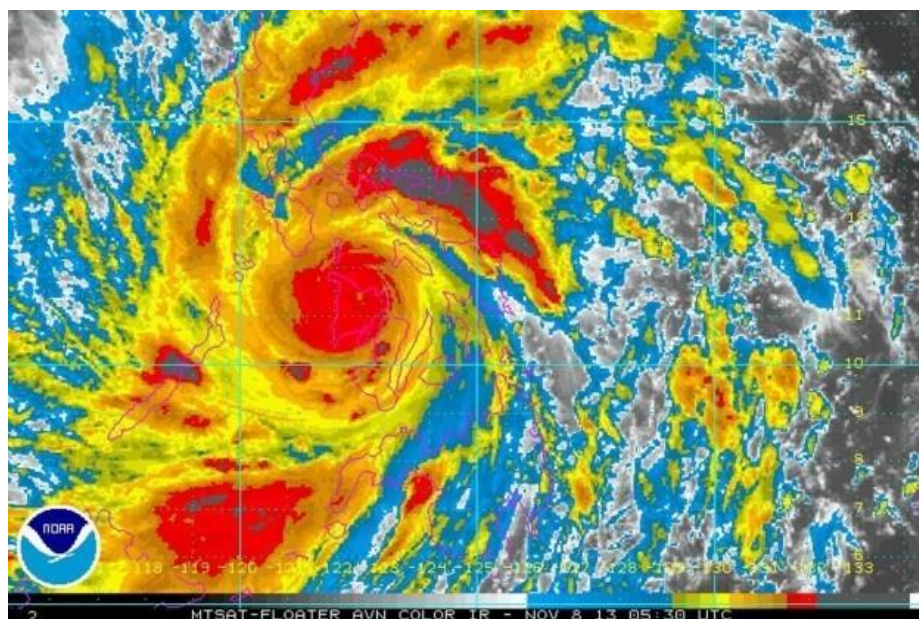


Figure 26. Rainfall analysis. Courtesy of NOAA.

Rapid weakening ensued as Haiyan approached its final landfall in Vietnam, ultimately striking the country when it was downgraded to severe tropical storm. Once onshore, the storm quickly diminished and was last noted as it dissipated over China during 11 November.

The coincident peak wind speeds occurring at landfall over the Philippines also helped to produce a significant storm surge, which was reported to be up to 5.2 meters (~17 feet) in Tacloban, located on the northeast tip of Leyte, where the strong cyclonic winds from Haiyan funneled water into the northwest corner of the Gulf of Leyte between the islands of Leyte and Samar.

In addition to the fierce winds and powerful surge, Haiyan brought copious amounts of rainfall to the central Philippines along with the Tropical Storm Thirty and another tropical disturbance, which all passed through the central Philippines within a ten day period (Figure 19). The combined rainfall analysis from these tropical cyclones (Figure 26) shows that most of the island of Leyte had rainfall totals greater than 500 mm (~19.7 inches, dark red) with a peak amount of over 685 mm (~27 inches, lighter purple) located over the southeast corner of the island¹⁶.

8. Typhoon Tip

The Typhoon Tip, the tropical storm affecting south east Asia in October 1979, is one of a very few exceptions to the general rule that hurricanes never reach a size comparable to an intense perturbation of the extra-tropical perturbations. It is considered to be the largest typhoon that ever occurred and one of the most intense typhoons as well.

Its formation mechanism, did not deviate from the standard over this region where the initial disturbance is triggered within the Monsoon trough, an area of the Inter Tropical Convergence Zone where minimum sea-level pressure occurs. This area of low-level vorticity is affected by significant low-level spin and marked by a better than average chance of

tropical cyclone formation due to their inherent rotation.

In the beginning this storm was slow to develop as the environmental circulation was heavily affected by the tropical storm Roger affecting the region roughly at the same time.

But after having lazily looped practically in place close to the Chuuk Islands it began a northwest motion on 8 October. Then the cyclone was very efficient in taking advantage of a concurrent upper tropospheric trough that favoured the upper level outflow of the cyclone and the remnant of the low-level circulation of the tropical storm Roger, the very same that damped its initial development. In view of that, it rapidly intensified and was upgraded to typhoon status on 9 October. Late on 10 October, the typhoon attained wind speeds equal to Category 4 strength on the Saffir-Simpson Hurricane Scale. By 11 October, Tip was a super typhoon with winds of at least 241 km/h (150 mph). From 9-11 October, the central pressure of the storm dropped 92 mbar and the typhoon's circulation expanded to a diameter of 2220 km with gale-force winds extending 1086 km from its center. The typhoon continued to intensify further, and early on 12 October reconnaissance aircraft recorded a worldwide record-low pressure of 870 mbar (870.0 hPa) with winds off 305 km/h when Tip was located about 840 km west-northwest of Guam (Figures 27-31).

¹⁶ See also <https://www.nasa.gov/content/goddard/haiyan-northwestern-pacific-ocean/#.VXmqovntmko>.

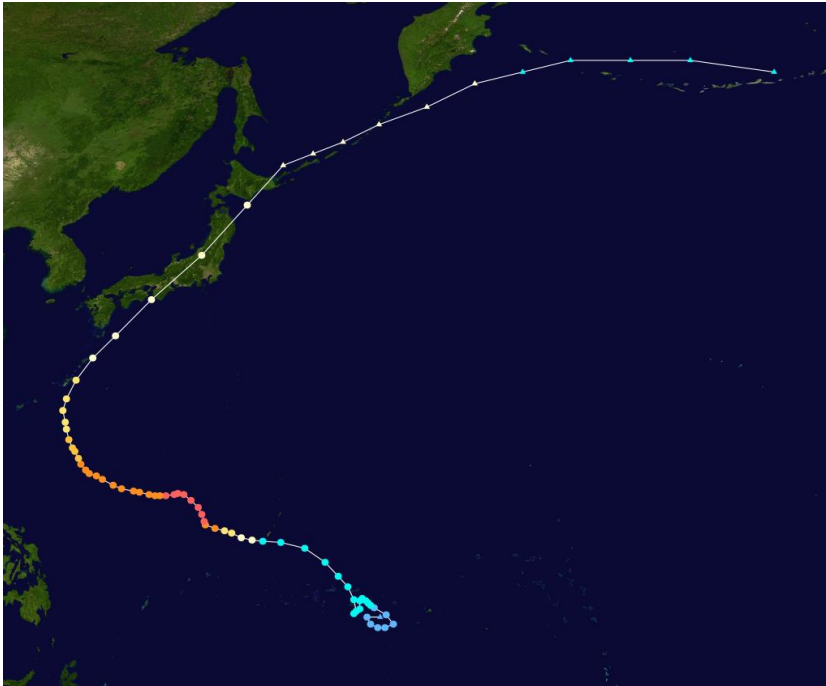


Figure 27. Ground track of the Typhoon Tip during its life. Courtesy of NOAA.

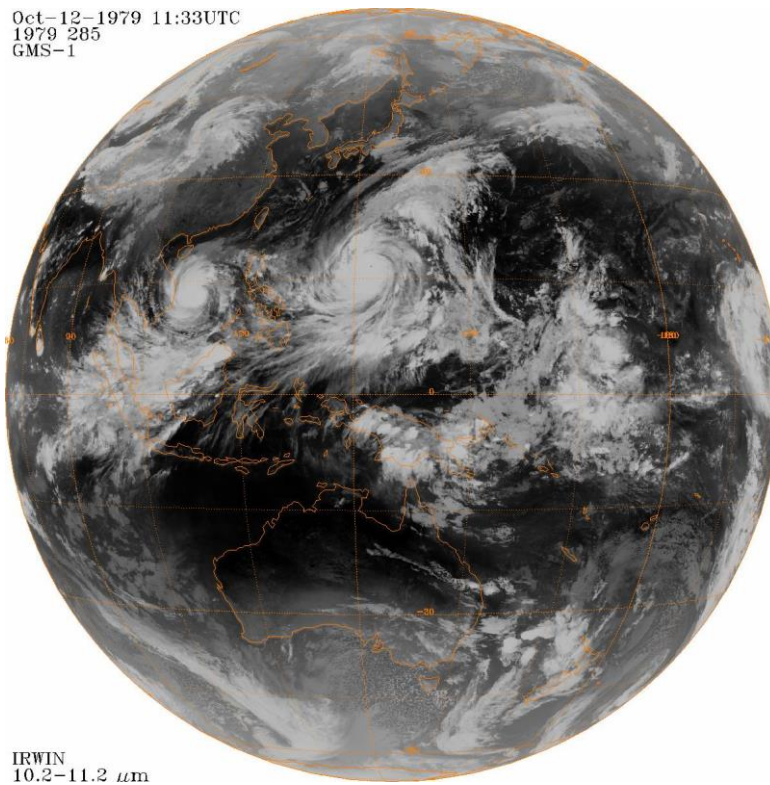


Figure 28. Full-disc satellite image regarding Typhoon Tip near its worldwide record peak intensity, in the western Pacific Ocean. Typhoon Sarah is formed to its west in the south China Sea. Courtesy of NOAA/NESDIS-NCDC/GIBBS. This full-disc image was acquired in the Thermal Infrared spectral band on 12 October 1979 by the Japanese geostationary meteorological satellite GMS-1 (Himawari-1). Courtesy of JMA.

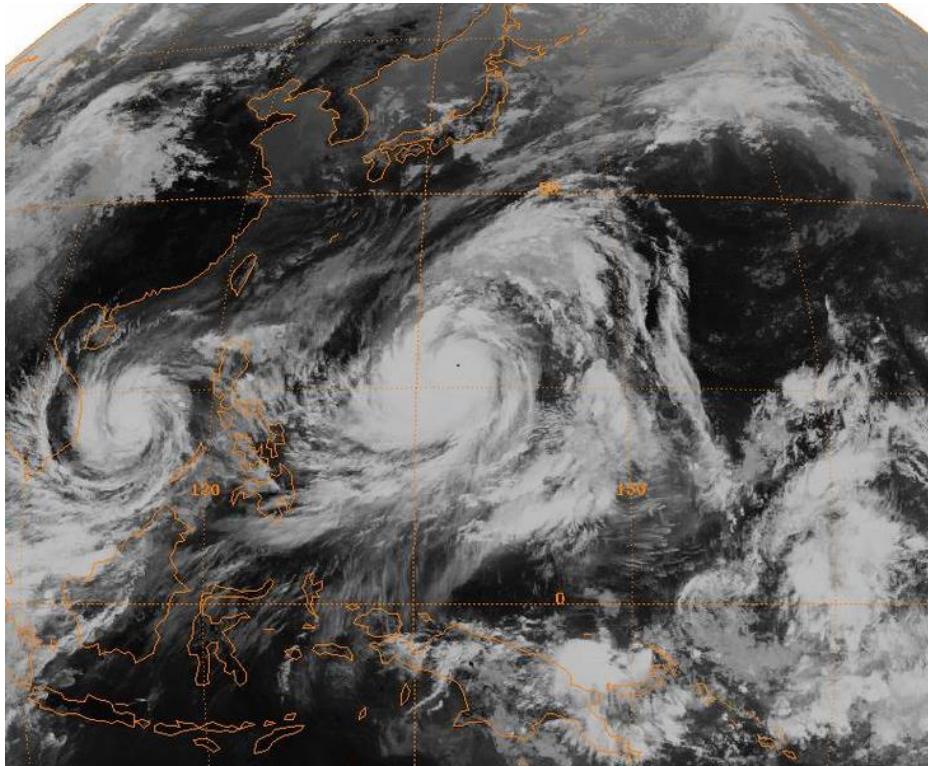


Figure 29. Enlargement of Figure 28 over the typhoons Sarah (left) and Tip (centre).

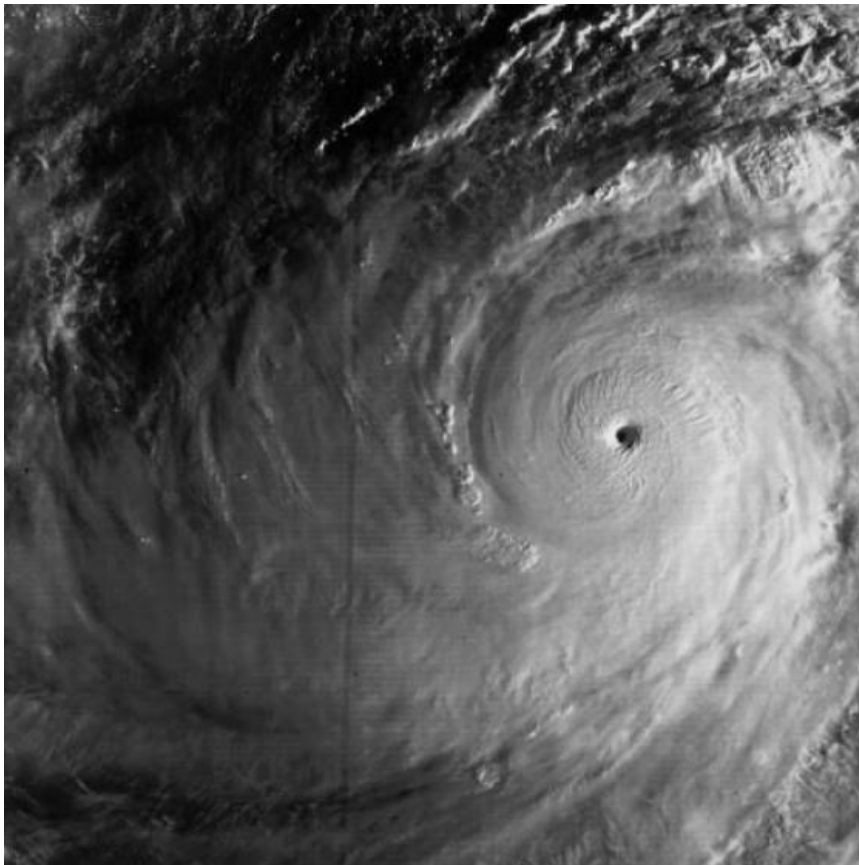


Figure 30. Typhoon Tip at peak intensity on 12 October 1979. Courtesy of NOAA.



Figure 31. Typhoon Tip observed on 14 October 1979 by the meteorological satellite TIROS-N flying in a quasi-polar sun-synchronous orbit. Courtesy of NOAA.

The typhoon Tip weakened after peaking with winds of 233 km/h (145 mph). It maintained this intensity for various days as it continued moving in a west-northwest direction. The typhoon then weakened further and curved toward the northeast on 17 October. A greatly weakened Typhoon Tip made landfall on Honshu, Japan, on 19 October with winds of 129 km/h. The storm quickly moved over the island and rapidly declined. It became extratropical over northern Honshu just hours after landfall and was last observed near the Aleutian Islands some time around 22 October¹⁷.

Acknowledgements

In this paper, M. Fea and M. Capaldo wrote paragraphs 1-2 and 6-8 integrating and looking in more detail at some aspects analysed in different documents of the: European Space Agency (ESA); National Oceanic and Atmospheric Administration (NOAA); Hurricanes: Science and Society (University of Rhode Island); World Meteorological Organization (WMO); National Aeronautics and Space Administration (NASA); Intergovernmental Panel for Climate

¹⁷ See <http://www.hurricanescience.org/history/storms/1970s/tip/>.

Change (IPCC); Japan Meteorological Agency (JMA); University of Hawaii; international literature and report; C. Pesaresi wrote paragraphs 3-5.

References

1. Antalovich J., "Disaster Response Aerial Remote Sensing Following Storms Irene and Lee", *Photogrammetric Engineering and Remote Sensing*, 77, 12, 2011, pp. 1185-1187.
2. Baker S.M., "Vulnerability and Resilience in Natural Disasters: A Marketing and Public Policy Perspective", *Journal of Public Policy & Marketing*, 28, 1, 2009, pp. 114-123.
3. Begum S., Alam S. and Ali S., "Cyclone Monitoring towards Disaster Management of Bangladesh", *Open Journal of Computer Sciences*, 1, 2, 2013, pp. 1-10.
4. Begum S., Nessa M. and Ali S., "Cyclone 'MOHASEN' monitored using remote sensing technology", *International Journal of Environmental Monitoring and Analysis*, 1, 3, 2013, pp. 95-98.
5. Bevis M. et al., "GPS Meteorology' Remote Sensing of Atmospheric Water Vapor Using the Global Positioning System", *Journal Of*

- Geophysical Research*, 97, 14, 1992, pp. 787-801.
6. Boutet Jr. J.C. and Weishampel J.F., "Spatial pattern analysis of pre- and post-hurricane forest canopy structure in North Carolina, USA", *Landscape Ecology*, 18, 2003, pp. 553-559.
 7. Chan P.W., "Measurement of turbulence intensity profile by a mini-sodar", *Meteorological Applications*, 15, 2, 2008, pp. 249-258.
 8. Chan P.W., "Observations of Tropical Cyclones by Remote-Sensing Instruments and Their Applications", in Veress B. and Szegedy J. (Eds.), *Horizons in Earth Science Research*, Nova Science Publishers, vol. 3, 2011, pp. 133-155.
 9. Chen Q., Wang L., Zhao H. and Douglass S.L., "Prediction of storm surges and wind waves on coastal highways in hurricane-prone areas", *Journal of Coastal Research*, 23, 2007, pp. 1304-1317.
 10. Clinch A.S., Russ E.R., Oliver R.C., Mitsova H. and Overton M.F., "Hurricane Irene and the Pea Island Breach: Pre-storm site characterization and storm surge estimation using geospatial technologies", *Shore & Beach*, 80, 2, 2012, pp. 1-10.
 11. Collins C.A., Evans D.L., Belli K.L. and Glass P.A., "Using Remotely Sensed Data and Elementary Analytical Techniques in Post-Katrina Mississippi to Examine Storm Damage Modeling", in Pye J.M., Rauscher H.M., Sands Y., Lee D.C. and Beatty J.S. (Eds.), *Advances in Threat Assessment and Their Application to Forest and Rangeland Management*, General Technical Report, PNW-GTR-802, vol. 1, 2010, pp. 225-236.
 12. Conner W.H., "Impact of hurricanes on forests of the Atlantic and Gulf Coasts, USA", in Laderman A.D. (Ed.), *Coastally Restricted Forests*, New York, Oxford University Press, 1998, pp. 271-277.
 13. Cutter S.L., Barnes L., Berry M., Burton C., Evans E., Tate E. and Webb J., "A place-based model for understanding community resilience to natural disasters", *Global Environmental Change*, 18, 2008, pp. 598-606.
 14. Dolfman M.L., Wasser S.F. and Bergman B., "The effects of Hurricane Katrina on the New Orleans economy", *Monthly Labor Review*, 2007, pp. 3-18.
 15. Dunnavan G.M. and Diercks J.W., "An Analysis of Super Typhoon Tip (October 1979)", 1980, *Monthly Weather Review*, 108, pp. 1915-1923.
 16. Durden S.L., "Remote Sensing and Modeling of Cyclone Monica near Peak Intensity", *Atmosphere*, 2010, 1, pp. 15-33.
 17. Emanuel K.A., "An Air-Sea Interaction Theory for Tropical Cyclones. Part I: Steady-State Maintenance", *Journal of the Atmospheric Sciences*, 43, 6, 1986, pp. 585-604.
 18. Emanuel K.A., "The dependence of hurricane intensity on climate", *Nature*, 326, 1987, pp. 483-485.
 19. Emanuel K.A., "Environmental Factors Affecting Tropical Cyclone Power Dissipation", *Journal of Climate*, 20, 2007, pp. 5497-5509.
 20. Emanuel K.A., "Anthropogenic Effects on Tropical Cyclone Activity", <http://wind.mit.edu/~emanuel/anthro.html>.
 21. Farris G.S., Smith G.J., Crane M.P., Demas C.R., Robbins L.L. and Lavoie D.L. (Eds.), *Science and the Storms: the USGS Response to the Hurricanes of 2005*, U.S. Geological Survey Circular 1306, 2007.
 22. Favretto A., "Progetti e strumenti a supporto della Geografia e della Cartografia: la 'terra digitale' ed i mappamondi virtuali", *Ambiente Società Territorio. Geografia nelle Scuole*, 2, 2009, pp. 15-20.
 23. Fea M., Giacomelli L., Pesaresi C. and Scandone R., "Remote sensing and interdisciplinary approach for studying volcano environment and activity", *Journal of Research and Didactics in Geography (J-READING)*, 1, 2, 2013a, pp. 151-182.
 24. Fea M., Minora U., Pesaresi C. and Smiraglia C., "Remote sensing and interdisciplinary approach for studying glaciers", in *Journal of Research and Didactics in Geography (J-READING)*, 2, 2, 2013b, pp. 115-142.
 25. Gesch D., "Topography-based Analysis of Hurricane Katrina Inundation of New Orleans", in Farris G.S., Smith G.J., Crane

- M.P., Demas C.R., Robbins L.L. and Lavoie D.L. (Eds.), *Science and the Storms: the USGS Response to the Hurricanes of 2005*, U.S. Geological Survey Circular 1306, 2007, pp. 53-56.
26. Gesch D., *Mapping and visualization of storm-surge dynamics for Hurricane Katrina and Hurricane Rita*, U.S. Geological Survey Scientific Investigations Report 2009-5230, 2009.
 27. Goldstein B.E., *Collaborative Resilience: Moving Through Crisis to Opportunity*, Cambridge, London, The MIT Press, 2012.
 28. Graham S. and Riebeek H., "Hurricanes, the greatest Storms on Earth", NASA Earth Observatory, 2006, <http://earthobservatory.nasa.gov/Features/Hurricanes/>.
 29. Harville E.W., Xiong X., Buekens P., Pridjian G. and Elkind-Hirsch K., "Resilience after Hurricane Katrina among pregnant and postpartum women", *Women's Health Issues*, 20, 1, 2010, pp. 1-15.
 30. Heitshusen B., *Analysis of Hurricane Sandy on Atlantic City, NJ*, Remote Sensing for the Geospatial Intelligence Professional: Fall 2012 Final Project, 2012.
 31. Holland G.J., "The maximum potential intensity of tropical cyclones", *Journal of the Atmospheric Sciences*, 54, 1997, pp. 2519-2541.
 32. Iacovelli D. and Vasquez T., "Super Typhoon Tip: Shattering all records", *Mariners Weather Log*, 42, 2, 1998, pp. 4-8.
 33. Jordan C.L., "On the influence of tropical cyclones on the sea surface temperature field", *Proceedings of the Symposium on Tropical Meteorology*, Wellington, New Zealand Meteorological Service, 1964.
 34. Kates R.W., Colten C.E., Laska S. and Leatherman S.P., "Reconstruction of New Orleans after Hurricane Katrina: A research perspective", *PNAS*, 103, 40, 2006, pp. 14653-14660.
 35. Katsaros K.B., Vachon P.W., Liu W.T. and Black P.G., "Microwave Remote Sensing of Tropical Cyclones from Space", *Journal of Oceanography*, 58, 2002, pp. 137-151.
 36. Kidder S.Q. et al., "Satellite analysis of tropical cyclones using the Advanced Microwave Sounding Unit", *Bulletin of the American Meteorological Society*, 2000, 81, pp. 1241-1259.
 37. Klemas V.V., "The role of remote sensing in predicting and assessing coastal storm impacts", *Journal of Coastal Research*, 25, 6, 2009, pp. 1264-1275.
 38. Klemas V.V., "Remote Sensing of Ocean Internal Waves: An Overview", *Journal of Coastal Research*, 28, 3, 2012, pp. 540-546.
 39. Knabb R.D., Rhome J.R. and Brown D.P., "Tropical Cyclone Report Hurricane Katrina", 2011, http://www.nhc.noaa.gov/data/tcr/AL122005_Katrina.pdf.
 40. Knutson T.R. et al., "Tropical cyclones and climate change", *Nature Geoscience*, 3, 2010, pp. 157-163.
 41. IPCC, *Climate Change 2013. The Physical Science Basis*, Cambridge, Cambridge University Press, 2013.
 42. Lam N.S.-N., Arenas H., Li Z. and Liu K.B., "An estimate of population impacted by climate change along the U.S. coast", *Journal of Coastal Research*, Special Issue 56, 2009, pp. 1522-1526.
 43. Lam N.S.-N., Liu K.-B., Liang W., Bianchette T.A. and Platt W.J., "Effects of Hurricanes on the Gulf Coast Ecosystems: A Remote Sensing Study of Land Cover Change around Weeks Bay, Alabama", *Journal of Coastal Research*, Special Issue 64, 2011, pp. 1707-1711.
 44. Lander M., Guard C. and Camargo S.J., "Super Typhoon Haiyan", *Bulletin of the American Meteorological Society* (Special Supplement), 95, 7, 2014, pp. S112-S114.
 45. Landsea C., "Why don't we try to destroy tropical cyclones by nuking them?", NOAA – Hurricane Research Division, <http://www.aoml.noaa.gov/hrd/tcfaq/C5c.html>.
 46. Marks F.D., "Hurricanes", 2003, http://curry.eas.gatech.edu/Courses/6140/ency/Chapter11/Ency_Atmos/Hurricanes.pdf.
 47. Metzl E.S., "The role of creative thinking in resilience after hurricane Katrina", *Psychology of Aesthetics, Creativity, and the Arts*, 3, 2, 2009, pp. 112-123.

48. Morin P., "Remote Sensing and Hurricane Katrina Relief Efforts", *Eos*, 86, 40, 2005, pp. 367-368.
49. Nayak S. and Zlatanova S. (Eds.), *Remote sensing and GIS technologies for monitoring and prediction of disasters*, Berlin, Springer, 2008.
50. Odow S., *Greatest Ever... Hurricanes and Typhoons*, Silas Odow, 2015.
51. Pelling M., *The Vulnerability of Cities. Natural Disasters and Social Resilience*, London, Earthscan, 2003.
52. Piñeros M.F., Ritchie E.A. and Tyo J.S., "Objective Measures of Tropical Cyclone Structure and Intensity Change From Remotely Sensed Infrared Image Data", *Geoscience and Remote Sensing*, 46, 11, 2008, pp. 3574-3580.
53. Plyer A., Liu A., Mizelle Jr. R.M. and Anglin R.V. (Eds.), *Resilience and Opportunity. Lessons from the U.S. Gulf Coast after Katrina and Rita*, Brookings Institution Press, 2011.
54. Powell M.D. et al., "Reconstruction of Hurricane Katrina's wind fields for storm surge and wave hindcasting", *Ocean Engineering*, 37, 2010, pp. 26-36.
55. Rana S., Gunasekara K., Hazarika M.K., Samarakoon L. and Siddiquee M., "Application of Remote Sensing and GIS for Cyclone Disaster Management in Coastal Area: A Case Study at Barguna District, Bangladesh", *International Archives of the Photogrammetry, Remote Sensing and Spatial Information Science*, XXXVIII, 2010, pp. 122-126.
56. REACH, *Haiyan Typhoon – The Philippines*, Final Assessment Report, 2014.
57. Rykhus R. and Lu Z., "Hurricane Katrina Flooding and Oil Slicks Mapped with Satellite Imagery", in Farris G.S., Smith G.J., Crane M.P., Demas C.R., Robbins L.L. and Lavoie D.L. (Eds.), *Science and the Storms: the USGS Response to the Hurricanes of 2005*, U.S. Geological Survey Circular 1306, 2007, pp. 49-52.
58. Saffir-Simpson Team, "The Saffir-Simpson Hurricane Wind Scale", 2012, <http://www.nhc.noaa.gov/pdf/sshws.pdf>.
59. Scowcroft G., Ginis I., Knowlton C., Yablonsky R. and Morin H., "Hurricanes: Science and Society", University of Rhode Island, 2011.
60. Smith J. and Rowland J., "Temporal Analysis of Floodwater Volumes in New Orleans After Hurricane Katrina", in Farris G.S., Smith G.J., Crane M.P., Demas C.R., Robbins L.L. and Lavoie D.L. (Eds.), *Science and the Storms: the USGS Response to the Hurricanes of 2005*, U.S. Geological Survey Circular 1306, 2007, pp. 57-60.
61. Stanturf J.A., Goodrick S.L. and Outcalt K.W., "Disturbance and coastal forests: a strategic approach to forest management in hurricane impact zones", *Forest Ecology and Management*, 250, 2007, pp. 119-135.
62. Storm Evolution and Energetics Research (SEER), "MET 200 Atmospheric Processes and Phenomena", <http://www.soest.hawaii.edu/MET/Faculty/businger/courses/met200.html>.
63. Turnipseed D.P., Wilson K.V., Stoker J. and Tyler D., "Mapping Hurricane Katrina peak storm surge in Alabama, Mississippi, and Louisiana", *Proceedings 37th Annual Mississippi Water Resources Conference*, 2007, pp. 202-207.
64. Wang W., Qu J.J., Hao X., Liu Y. and Stanturf J.A., "Post-hurricane forest damage assessment using satellite remote sensing", *Agricultural and Forest Meteorology*, 150, 2010, pp. 122-132.
65. Womble J.A., Ghosh S., Adams B.J. and Friedland C.J., *Advanced Damage Detection for Hurricane Katrina: Integrating Remote Sensing and VIEWSTM Field Reconnaissance*, MCEER Special Report Series Engineering and Organizational Issues Before, During and After Hurricane Katrina, vol. 2, 2006.
66. Zhu T. and Weng F., "Hurricane Sandy warm-core structure observed from advanced Technology Microwave Sounder", *Geophysical Research Letters*, 40, 12, 2013, pp. 3325-3330.